

MONITORING AND CONTROL OF SMART WELLS

**A REPORT SUBMITTED TO THE DEPARTMENT OF
ENERGY RESOURCES ENGINEERING**

OF STANFORD UNIVERSITY

**IN PARTIAL FULFILLMENT OF THE REQUIREMENTS
FOR THE DEGREE OF MASTER OF SCIENCE**

**By
Zeid M. Al-Ghareeb
June 2009**

©Copyrights by Zeid Alghareeb 2009

All Rights Reserved

I certify that I have read this report and that in my opinion it is fully adequate, in scope and in quality, as partial fulfillment of the degree of Master of Science in Petroleum Engineering.

Prof. Roland Horne
(Principal Advisor)

Abstract

Smart wells, wells equipped with smart completion, provide great potential to improve the recovery from hydrocarbon resources. Smart wells provide the ability to control uncertainties associated with reservoir heterogeneity. One example is to mitigate unexpected water production due to fractures and hence increase the ultimate recovery. This is achieved by selectively controlling production from multiple laterals. Due to subsurface communication between laterals that have different productivity indices, it is difficult in practice to optimize production from smart wells. The optimization of smart wells involves more than one parameter. These parameters include the settings of the downhole inflow control valves (ICV) that act as a subsurface chokes.

This research focused on the reservoir engineering aspects of finding the optimum ICV configuration that optimizes reservoir performance parameters such as recovery factor and net present value. Also, the work studied the effect of heterogeneity, mainly fractures, on the optimization process. This research also proposed a technique to quantify the effect of fractures on the optimization process to provide recommendations of further analysis.

Genetic algorithm (GA) was used as the main optimization engine to find the optimum ICV configuration. The GA was accompanied by a data library (proxy) to reduce the number of required simulation runs. The commercial reservoir simulator Eclipse was used as the objective function evaluator that assesses how good an ICV configuration is.

Several examples are presented to show the improvement in reservoir parameters made using the optimization process. These examples include a synthetic model, and real onshore and offshore models. Various objective functions were optimized such as water cut minimization, and net present value maximization.

Acknowledgment

First and foremost, I would like to express my sincere gratitude and appreciation to my advisor Prof. Roland Horne. His guidance, inspiration, and insights made this work possible. His wide knowledge, expert advice, and charming way of teaching are beyond description and will be of great value to me.

I would like to also thank my colleagues Obi Isebor for helping me with setting up the genetic algorithm main routine, Jerome Onwunalu for the many useful suggestions, and my two officemates Alejandro and Mike for the great company during the many late nights of studying. My special thanks go to the small Saudi community at Stanford for the priceless gatherings during the two years.

I am indebted to my mentor at Saudi Aramco Mr. Shamsuddin Shenawi for allowing me to be an additional burden in his busy schedule. Thanks go to my superiors Mr. Saad Al-Garni, Mr. Methgal Al-Shammari, and Mr. Bevan Yuen for providing me with all help and logistic support.

I also must thank my parents. They taught me many important lessons in my life and gave me all their love and support through every stage of my life and my education. I am very grateful to them. I also need to thank my older brother Fahad for the invaluable advice and the entertaining conversations from Australia.

Lastly and mostly, all love and appreciation go to my wife Mariam and my son Mohammed for showering me with all the love and support during the difficult times. Coming home to see them everyday was all I needed. This work is dedicated to them.

Table of Contents

Abstract	vii
Acknowledgment	ix
List of Figures	xiii
List of Tables	xv
1. Introduction	1
1.1. General Background	1
1.2. Literature Survey.....	4
1.3. Problem Description.....	5
2. Optimization Tools	7
2.1. Genetic Algorithm	7
2.1.1. Terminology.....	8
2.1.2. Genetic Algorithm Engine	11
2.1.3. GA Solution Representation	11
2.1.3.1. GA Encoding Example	12
2.2. Numerical Reservoir Simulator.....	15
2.2.1. Multilateral Wells Representation.....	15
2.2.2. ICV Representation.....	16
2.3. ICV Design	19
2.4. Optimization Framework	20
3. Applications on Various Reservoir Models	23
3.1. Synthetic Model – Water Cut Minimization.....	23
3.1.1. The Synthetic Model	23
3.1.2. Optimum ICV Setting – Water Cut Minimization	27

3.2. Offshore Model – Net Present Value Maximization.....	29
3.2.1. The Offshore Model.....	29
3.2.2. Optimum ICV Setting – NPV Maximization	33
3.3. Onshore Model – Production Plateau	38
3.3.1. The Onshore Model	38
3.3.2. Optimum ICV Setting – Production Plateau	42
4. Fractures Effects on Smart Wells Optimization.....	47
4.1. Fracture Representation.....	50
4.2. Fracture Location Study	52
4.3. Fracture Location Study Framework.....	53
4.4. Onshore Model Fracture Study – Case One	54
4.4.1. Onshore Model – Case 1a	56
4.4.2. Onshore Model – Case 1b	56
4.5. Onshore Model Fracture Study – Case Two	57
4.5.1. Onshore Model - Case 2a	58
4.5.2. Onshore Model – Case 2b	59
5. Conclusions and Future Work.....	61
5.1. Conclusions.....	61
5.2. Future Work.....	62
Nomenclature	63
Bibliography	65
Appendix A.....	67
Appendix B.....	70

List of Figures

Figure 1-1: Schematic of components of a multilateral smart well (Dumville, 2008)	2
Figure 1-2: Production target achieved by a lower number of smart wells (Mubarak et al., 2007).....	2
Figure 2-1: Decimal and binary individuals	8
Figure 2-2: Presentation of generations within GA.....	8
Figure 2-3: Transition from one generation to the next	10
Figure 2-4: Crossover operator	10
Figure 2-5: Mutation operator	10
Figure 2-6: Binary form of solution	12
Figure 2-7: Fitness value for continuous and binary encodings	14
Figure 2-8: Average fitness value vs. generation	14
Figure 2-9: Structure of keyword WSEG with two laterals emanating from the motherbore	16
Figure 2-10: Eclipse ICV file	18
Figure 2-11: Flowchart of the optimization framework	22
Figure 3-1: Synthetic model permeability distribution and producer location	25
Figure 3-2: Oil flow rate vs. ICV setting when only one lateral is producing	26
Figure 3-3: oil flow rate vs. ICV setting when all laterals are producing	27
Figure 3-4: Solution surface with lateral two kept at fully open position	28
Figure 3-5: Progress of GA optimization for the Synthetic model	29
Figure 3-6: Offshore model 3D grid structure and initial water saturation	30
Figure 3-7: Offshore model - permeability distribution of layer nine.....	32
Figure 3-8: Offshore model - production rate and water cut (base case).....	33
Figure 3-9: Offshore model - individual lateral production rate (base case)	34
Figure 3-10: Offshore model - individual lateral water cut (base case).....	34
Figure 3-11: Solution surface with lateral-0 (MB) fully closed	35

Figure 3-12: Progress of GA optimization for the offshore model.....	36
Figure 3-13: Offshore model - production rate and water cut (optimized case)	37
Figure 3-14: Offshore model - individual lateral production rate (optimized case)	37
Figure 3-15: Onshore model 3D grid structure and initial water saturation.....	39
Figure 3-16: Onshore model – five-spot pattern on saturation map.....	41
Figure 3-17: Onshore model – production rate and water cut (base case)	44
Figure 3-18: Onshore model - individual lateral production rate (base case)	44
Figure 3-19: Onshore model – production rate and water cut (optimized case).....	45
Figure 3-20: Onshore model - individual lateral production rate (optimized case)	45
Figure 4-1: Fractures and matrix in reservoir (Warren and Root, 1963)	47
Figure 4-2: Fracture imaging log showing fracture spacing, formation orientation, and dip	49
Figure 4-3: Source model technique as discrete fracture (Voelker, 2004)	50
Figure 4-4: Source model representation as a curved fracture (Voelker, 2004).....	51
Figure 4-5: Multiple realizations comprising an area of possible fracture location	52
Figure 4-6: Framework of fracture location study.....	53
Figure 4-7: location of study areas in Case 1a and Case 1b.....	55
Figure 4-8: Onshore model - permeability and porosity of Case 1a and Case 1b...	55
Figure 4-9: location of study areas in Case 2a and Case 2b.....	57
Figure 4-10: Onshore model - permeability and porosity of case 2a and case 2b...	58

List of Tables

Table 2-1: MATLAB GA Toolbox options	11
Table 2-2: Summary of problem parameters	13
Table 3-1: Synthetic model - reservoir and rock properties	24
Table 3-2: Synthetic model - fluid properties.....	24
Table 3-3: Areas corresponding to ICV settings for the synthetic models.....	26
Table 3-4: Offshore model - reservoir and rock properties	30
Table 3-5: Offshore model – fluid properties	31
Table 3-6: Areas corresponding to ICV settings for the offshore models.....	32
Table 3-7: Onshore model - reservoir and rock properties	39
Table 3-8: Onshore model – fluid properties.....	40
Table 3-9: Onshore model - production well properties.....	41
Table 3-10: Areas corresponding to ICV settings for the onshore model.....	42
Table 4-1: Comparison of fracture location effect – case 1a	56
Table 4-2: Comparison of fracture location effect – case 1b	57
Table 4-3: Comparison of fracture location effect – case 2a	59
Table 4-4: Comparison of fracture location effect – case 2b	59

CHAPTER 1

1. Introduction

1.1. General Background

Well design and planning has advanced during the last two decades, from conventional vertical wells to nonconventional horizontal wells (NCWs) using directional drilling technology. Nonconventional wells range from simple horizontal wells with single wellbore to complex multilaterals even with multiple sublaterals (fishbone wells).

Nonconventional wells offer more cost-effective alternatives to conventional wells in terms of drilling, completion, surface equipment, and long-term operation costs. Production targets are achieved with a far smaller number of nonconventional wells as they provide better reservoir exposure. From a reservoir management point of view, nonconventional wells improve productivity index (PI) by maximizing reservoir contact, minimizing water coning by operating at lower drawdown, and increasing sweep efficiency by redistributing production along the horizontal section.

A ‘smart’ or ‘intelligent’ well is considered one of the most advanced types of nonconventional wells. A typical smart well is equipped with a special completion that has packers or sealing elements which allow partitioning of the wellbore, pressure and temperature sensors and downhole inflow control valves (ICV) installed on the production tubing, Figure 1-1. The sensors allow continuous monitoring of pressure and temperature while the ICVs provide the flexibility of controlling each branch of a multilateral well independently. A smart well can be either a multilateral well where every lateral is controlled by an ICV or a single bore well where each segment is controlled by an ICV.

Most of the recent oil and gas fields developments in Saudi Arabia are furnished with smart wells. They provide the desired production target with lower capital and operating costs. Figure 1-2 shows a comparison between vertical, horizontal, and smart wells that were deployed in different developments within the same field. 48 smart wells achieved the desired production target as opposed to 150 vertical wells. (Mubarak, Pham, Shamrani, and Shafiq, 2007)

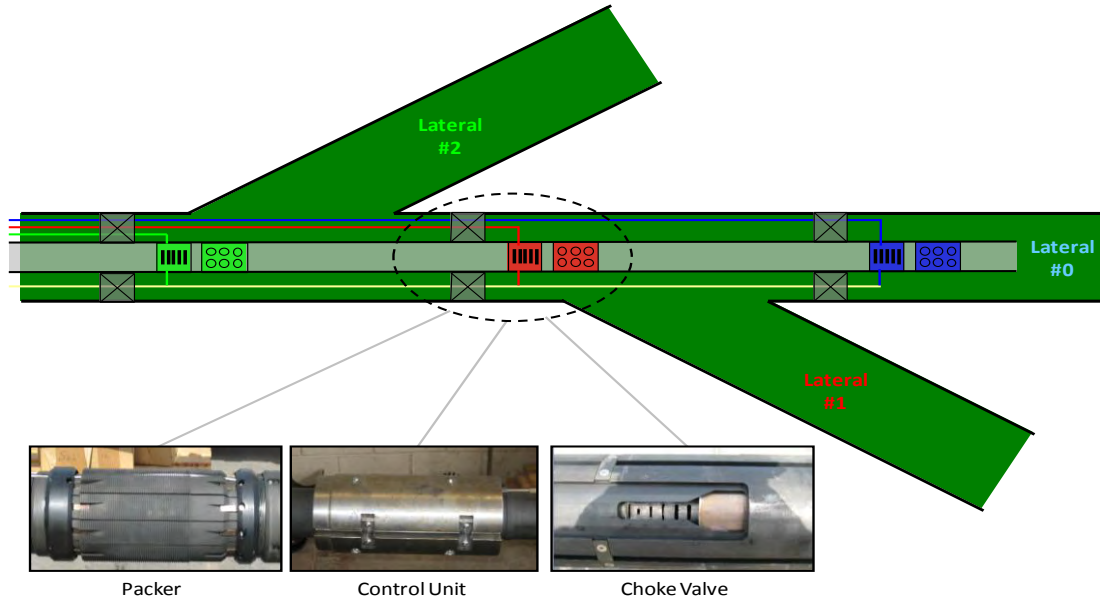


Figure 1-1: Schematic of components of a multilateral smart well (Dumville, 2008)

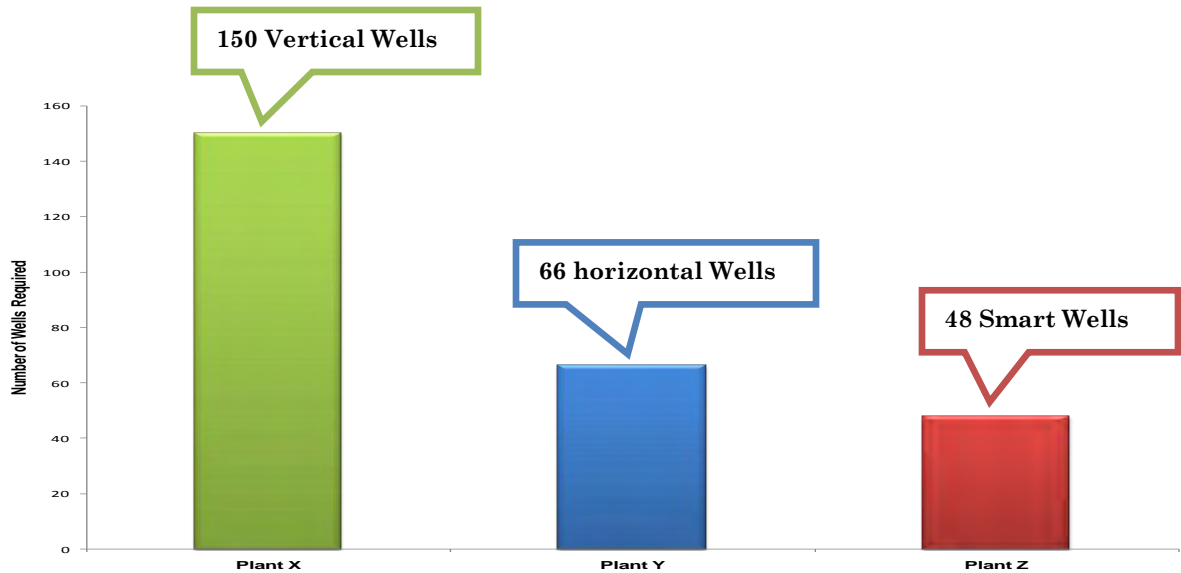


Figure 1-2: Production target achieved by a lower number of smart wells (Mubarak et al., 2007)

The advantages of smart wells have been demonstrated in practical applications for both single and multiple reservoir production (non-commingled production). Because of their ability to control production from each lateral or segment through ICV adjustment and manipulation, smart wells can mitigate water production by allocating the optimum production rate and therefore increase the ultimate recovery.

Unlike conventional wells where only surface control is used to determine the optimum production rate, optimization of smart wells requires determining the best combination of ICV settings (ICV configuration) that yields the highest recovery factor and hence profit. In the case of commingled production, laterals or branches are in contact with each other within the immediate vicinity of the reservoir. This adds another dimension to the optimization process as one lateral might affect the production of other laterals (in the case of water breakthrough).

Reservoir engineering practices follow two approaches in optimizing oil production from smart wells. These approaches are the reactive approach and the proactive approach. The reactive approach is usually achieved on a trial and error basis, making decisions based on current conditions. A series of production tests is made to determine the best ICV configuration. A portable multiphase flow meter (MPFM) is usually used for a faster decision. The reactive approach mainly corrects for any deviation from the production target; i.e. fast increase in water cut due to heterogeneity. On the other hand, a proactive approach uses an optimization algorithm to achieve the best ICV configuration that yields maximum oil recovery over a period of time in particular making estimates of future events. The proactive approach also takes advantage of the availability of real time production data which allows for better decisions. Although the reactive approach is very successful in correcting deviations from production target as they happen, it may not result in maximum oil recovery.

The main objective of this study was to propose an optimization technique as a proactive approach to optimize the production from smart wells. The optimization technique entails the use of genetic algorithm, applied in conjunction with a commercial reservoir simulator that is capable of modeling ICVs. This study also assessed the value of knowing fracture locations and their effect on the optimum ICV settings.

1.2. Literature Survey

Various reactive procedures and proactive techniques have been proposed to optimize production from smart wells. Mubarak, Pham, Shamrani, and Shafiq (2007) performed an intensive production test as a reactive measure to eliminate water production from a trilateral smart well. Although their production test procedure was determined based on their observations in the field, some interesting results and observations that could be considered in a proactive approach have been revealed. Among these observations was the laterals' sensitivity to the ICV setting. In one lateral, a low ICV setting completely eliminated water production as the water production was a result of water coning through nearby vertical fracture. On the other hand, a low ICV setting slightly reduced water production in another lateral and shut-in of that lateral was necessary as the source of water in this case was the advanced water injection flood front. Jalali, Bussear, and Sharma (1998) successfully increased the deliverability of a smart gas well drilled in a two-layer system by producing the top layer without downhole restriction and gradually unchoking the bottom layer as the bottom hole pressure declined.

Yeten, Durlofsky and Aziz (2002) described a gradient-based technique to maximize cumulative oil recovery from smart wells. Their optimization technique was performed over discretized time steps to ensure that earlier ICV settings determined for earlier time steps would not have negative effects at later time. Naus, Dolle, and Jansen (2006) proposed a workflow in which a production engineer can determine the change in flow rate as a result of a change in the ICV setting.

The workflow used an algorithm that required instantaneous and derivative information. The performance of their algorithm was tested in two reservoir cases with the objective of maximizing ultimate recovery. The optimization resulted in accelerated production but not necessarily higher ultimate recovery. Brouwer and Jansen (2002) investigated the impacts of smart completions with different well targets and constraints; i.e. BHP or liquid rate using optimal control theory. Their results showed that wells operating with rate control have the ability to accelerate production and increase ultimate recovery. Alhuthali, Datta-Gupta, Yuen, and Fontanilla (2009) presented waterflood optimization using smart wells and optimal rate control. Their approach relied on equalizing the streamline time of flight at the producing wells to maximize sweep efficiency. Yeten (2003) proposed a general methodology to optimize the type of nonconventional well, trajectory, location, and ICV setting. His method was based on genetic algorithm coupled with hill climbing and artificial neural networks.

1.3. Problem Description

A smart well is best drilled in reservoirs where wellbore hydraulics (water coning or cusping) and heterogeneity (fractures causing early water breakthrough) exist. Therefore, eliminating water coning and delaying water breakthrough by determining the best ICV configuration provides considerable scope for improving oil and gas production. This study used stochastic methods such as genetic algorithm to find the optimum ICV configuration. In addition, this study investigated the effect of heterogeneity, mainly fractures, on the optimization technique. As mentioned earlier, the laterals or segments of smart wells might be in contact with each other within the reservoir. This indicates that if one lateral experiences an early water breakthrough due to fractures existence, the overall production from the well will be affected.

CHAPTER 2

2. Optimization Tools

2.1. Genetic Algorithm

Genetic algorithm (GA) was first described by John Holland in 1975 and developed by him, his students, and his colleagues. The algorithm is modeled on the principle of evolution via natural selection (Goldberg, 1989). GA search is based on combining survival of the fittest with random information exchange. GA is considered a global optimization method that only uses the objective function value (*fitness*) as a source of evaluation instead of using derivative or gradient information to guide the search. GA searches the solution domain by creating a random set (*initial generation*) of binary strings (*individuals*). GA continues to span the solution domain by introducing new sets of artificial strings using bits and pieces of the fittest *individuals* from previous generations. Unlike other methods, GA uses probabilistic transition rules to guide the search.

GA was chosen as the optimization tool to find the optimum ICV configuration because it is:

- a global search method that is applicable for functions with local optima;
- applicable for discontinuous functions where derivatives can not be obtained;
- well-suited for parallel computation which increases the optimization speed;
- easy to hybridize with other optimization algorithms.

2.1.1. Terminology

Before we discuss how genetic algorithm works, it is essential to introduce some basic terminology of GA that will be mentioned extensively in this report.

Individual: an individual is a member of a population that contains a potential solution to the optimization problem. An individual can be represented as a binary string or a decimal string, Figure 2-1. Both the decimal string and the binary string shown in Figure 2-1 carry the same information. Assuming that every three bits in the binary string represent a decimal number, we get $V_1 = 5$, $V_2 = 2$, $V_3 = 6$.

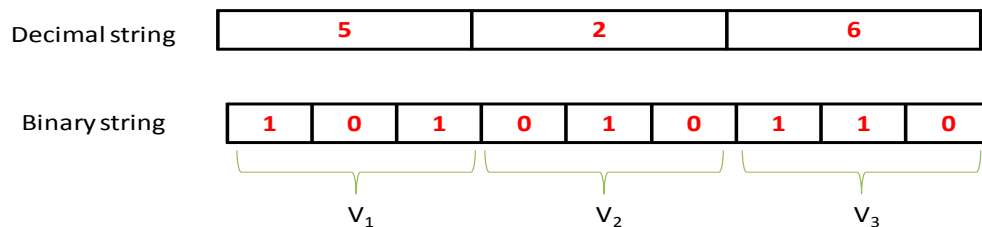


Figure 2-1: Decimal and binary individuals

Population size: if a population size is three, then three *individuals* will be grouped together to form a *population*.

Generation: is a term that indicates an iteration to be taken within the GA. Each generation contains a predefined *population size*, Figure 2-2 . The larger the number of generations, the higher the probability that the GA will find the optimum point in the search domain. The cost of optimization increases as the number of generations increases.

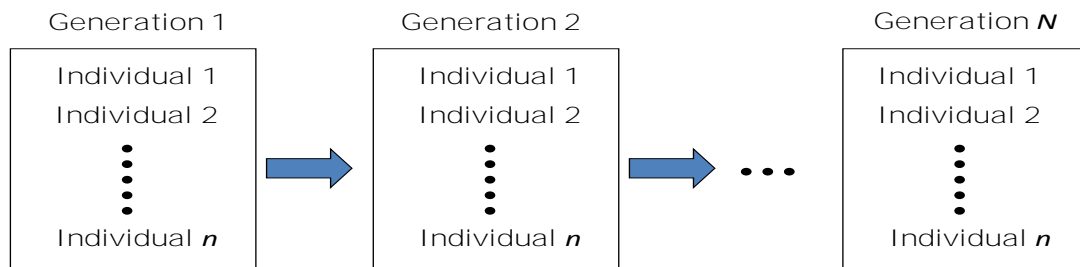


Figure 2-2: Presentation of generations within GA

Fitness score: is assigned to each *individual* according to how good the solution carried by the *individual* is. For example, the fitness may be represented as the oil production if we are trying to maximize oil recovery. The highly fit *individuals* (high *fitness score*) are given more opportunities to “reproduce”. The least fit *individuals* on the other hand are less likely to get selected for reproduction, and therefore die out.

Elitism: is a concept in GA which indicates that the best *individual* in a population is replicated into the next population without any alteration. The use of elitism guarantees that the best individual will not be degraded by the process of mutation or crossover.

Parents: are a couple of *individuals* that are selected based on their fitness score and mated to produce new *offspring* to replace lower fitness score *individuals* in the next generation.

Offspring: are *individuals* that are created as a result of mating two parents. *Offspring* share some features taken from both parents.

Selection: is a sampling process applied to the current *generation* to create an intermediate *generation*. *Crossover* and *mutation* are applied to the intermediate *population* to create the next *population*, Figure 2-3.

Crossover: is one of three operators that result in creating new *individuals*. *Crossover* is applied randomly to paired *individuals* (*parents*) with a probability p_c to form two new *offspring* that are inserted into the next generation, Figure 2-4. Prior to *crossover*, the population is shuffled by the selection process.

Mutation: is responsible for flipping a bit in one or more individuals within the *population*, when a random drawn value is less than the *mutation* probability p_m , Figure 2-5. *Mutation* probability is typically between 0.1% - 1.0%. *Mutation* is applied after *crossover*.

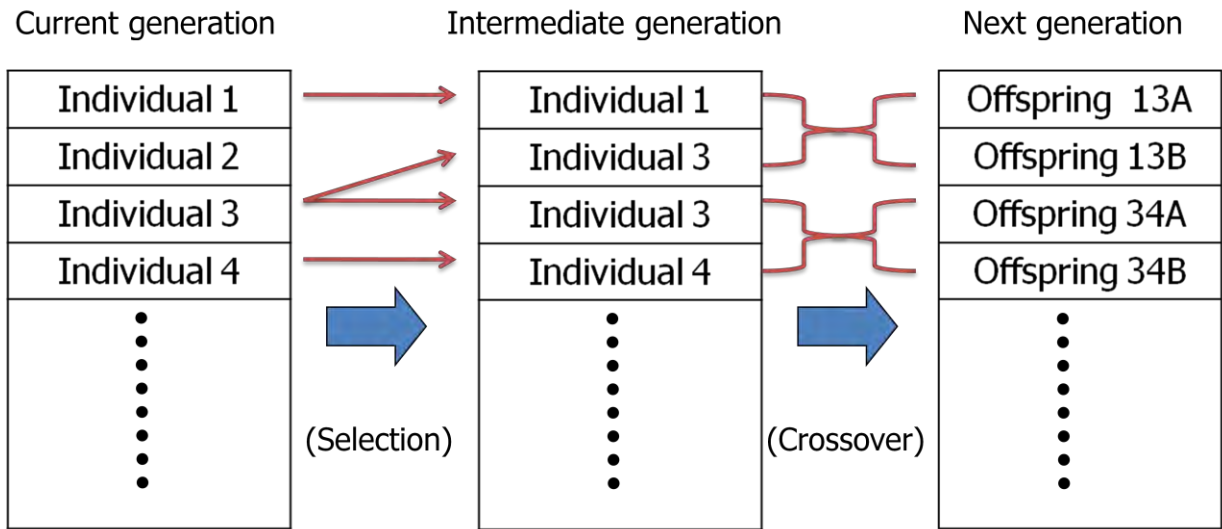


Figure 2-3: Transition from one generation to the next

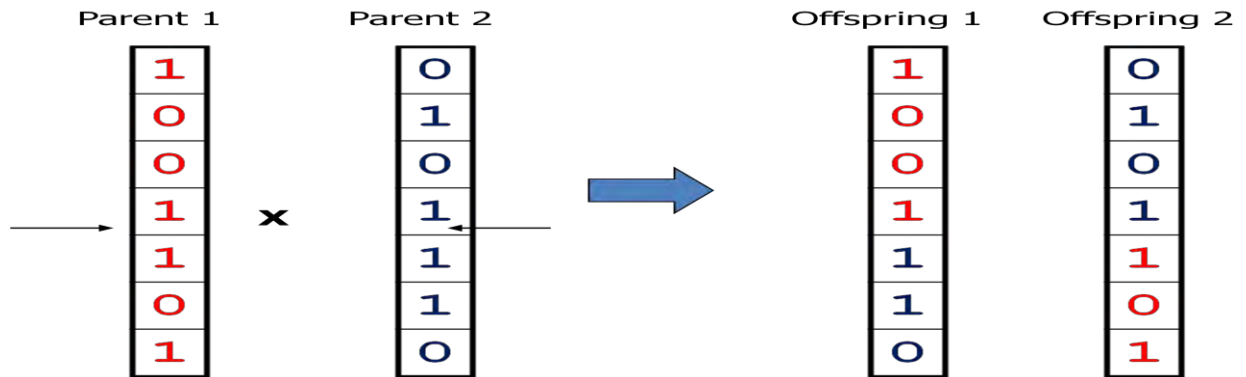


Figure 2-4: Crossover operator

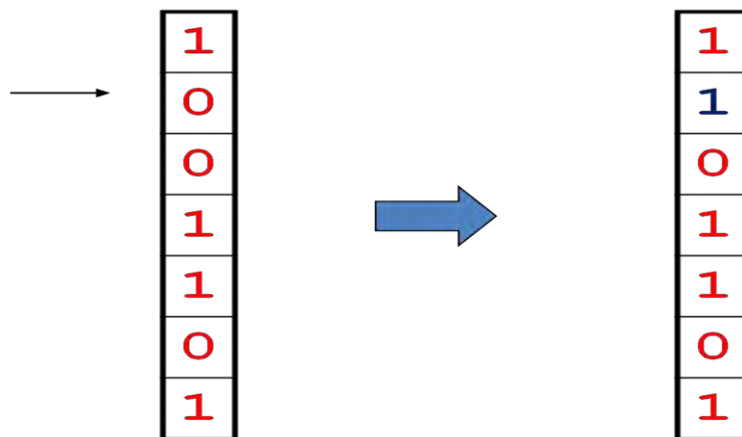


Figure 2-5: Mutation operator

2.1.2. Genetic Algorithm Engine

MATLAB® Genetic Algorithm Toolbox, part of MATLAB Optimization Toolbox, was the main optimization engine used for this problem. The GA Toolbox is closely integrated with other optimization tools such as pattern search, conjugate gradient, and steepest descent. GA can be used to find a good starting point to an optimization problem for instance while pattern search can improve the quality of the solution. The GA Toolbox features a graphical user interface, the ability to solve constrained problems, the flexibility to modify and create selection, crossover, and mutation functions, and the capability for parallelization (“Genetic Algorithm and Direct Search Toolbox 2”).

Table 2-1: MATLAB GA Toolbox options

Function	MATLAB GA Toolbox options
Creation	Uniform
Fitness Scaling	Rank-based, proportional, linear scaling
Selection	Roulette, stochastic uniform, tournament
Crossover	Arithmetic, scattered, heuristic, single-point
Mutation	Adaptive, feasible, Gaussian, uniform
Plotting	Best fitness, best individual, selection index

2.1.3. GA Solution Representation

Before GA can be run, a suitable coding or representation for a potential solution to an optimization problem must be devised. It is useful to represent the solution as a set of parameters that are joined together to form a string of values. GA MATLAB offers two types of solution forms depending on the type of problem:

Binary form

Binary form represents variables in binary space using 0’s and 1’s. It is suitable for discontinuous problems such as ICV configuration problems where an ICV cannot be open at position 2.316 for example. Binary forms run faster than other forms of

coding because the solution can only be represented by integers. Binary forms require decoding the variables before using them in the objective function. Binary forms are superior to other forms of encoding when the possible solution boundary is large.

Real form

Real form is a more intuitive process. It does not require decoding and it is suitable for problems where the solution is a real number; i.e. production well rate optimization. Continuous forms require a larger population size to search the bigger solution space and therefore it takes longer time.

2.1.3.1. GA Encoding Example

In this section, the MATLAB GA Toolbox will be illustrated by finding the minimum point of a simple quadratic equation to compare the performance of the binary and continuous forms of encoding.

$$\begin{aligned} \min f(x) &= 2x^2 - 4x \\ \text{st: } 0 &\leq x \leq 7 \end{aligned} \tag{2.1}$$

In order to represent the solution in the binary form, the maximum number of bits in the solution string should be determined. Here, we know that the minimum value for the variable is zero while the maximum is seven. Since seven can be represented using three bits, the minimum number of bits in the string representing this problem’s solution should be at least three, Figure 2-6.

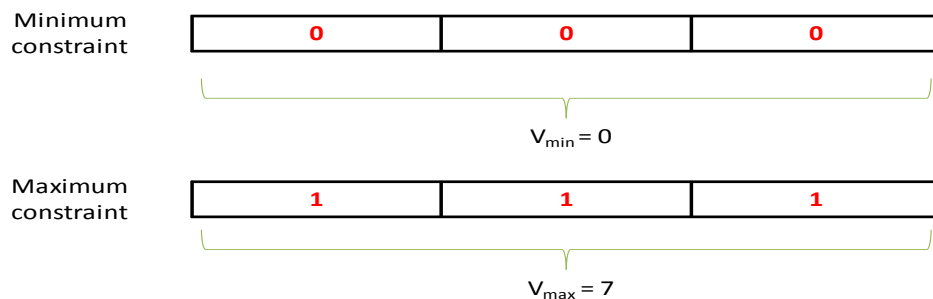


Figure 2-6: Binary form of solution

On the other hand, the continuous form does not require any sort of encoding and can be simply represented as any number between the minimum and maximum constraints.

Table 2-2: Summary of problem parameters

Parameter	Option
Population size	9
Generation number	3
Elite count	1
Crossover function	Scattered
Crossover fraction	0.8
Mutation function	Gaussian
Selection function	Stochastic uniform

In order to fairly compare the two forms of encoding, the optimization is repeated ten times for each form. Figure 2-7 shows the optimization solution (fitness value) for both forms of encoding. It is worth noting that the success rate of the binary encoding was 70% while the success rate of the continuous encoding was only 10%. Seven out of ten trials succeeded in finding the true minimum when using binary encoding (blue bars in Figure 2-7), whereas only one out of ten succeeded when using continuous encoding (red bars in Figure 2-7). It is likely that the continuous encoding may have achieved more successes if has more generations been computed, although this would have been at greater computational cost. Figure 2-8 shows the average fitness value for all generations for both forms of encoding. Although, both the binary and continuous forms are converging toward the actual minimum *fitness value* as generations are formed, Figure 2-8 gives a clear indication that the quality of generations in the binary form is superior (average fitness value is always closer to the true minimum fitness value).

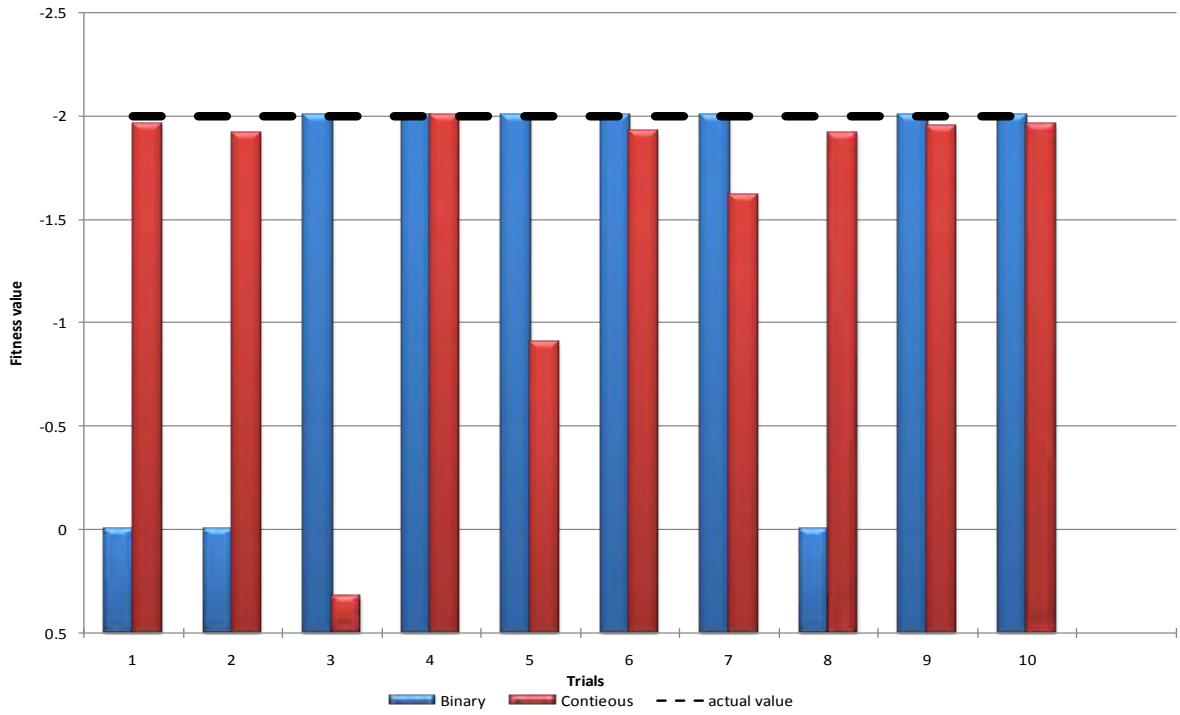


Figure 2-7: Fitness value for continuous and binary encodings

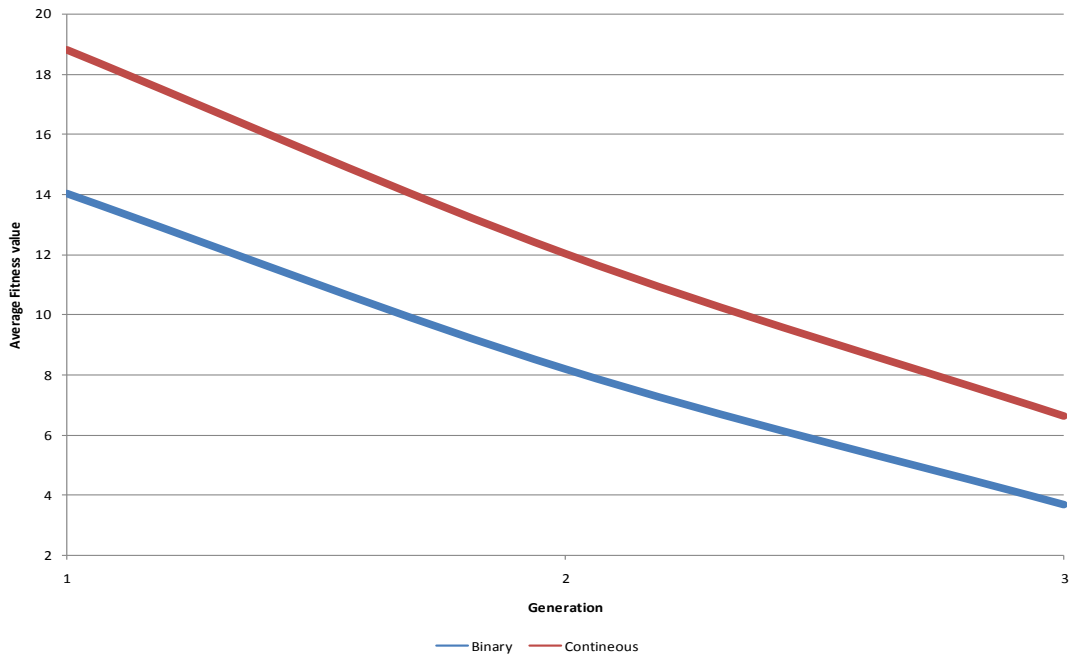


Figure 2-8: Average fitness value vs. generation

2.2. Numerical Reservoir Simulator

Schlumberger GeoQuest's `Eclipse` was used as the numerical reservoir simulator in this research. `Eclipse` can easily implement many types of production and economic constraints through its existing keywords. These constraints include economic production limit, production rate limit, and bottom hole pressure limit (BHP). `Eclipse` will evaluate the objective function that determines how good an ICV configuration is. A communication between `Eclipse` and GA MATLAB was established so that `Eclipse` can evaluate the proposed configuration of ICVs and send the results back to GA MATLAB to proceed further in the optimization process. However, before we explain how `Eclipse` communicates with GA MATLAB, it is crucial to discuss the important keywords used in `Eclipse` to represent a multilateral well and ICVs.

2.2.1. Multilateral Wells Representation

`Eclipse` has the capability to model multilateral wells via the keyword `WSEGS`. `WSEGS` can be used to represent a single well with multiple segments or a multilateral well with horizontal branches. If a multilateral well is desired, the point in the motherbore at which a new branch emanates should be defined, Figure 2-9. Although not discussed in this report, special care should be taken when a branch is not completed at the center of the reservoir grid blocks. Proper well index values (WI) must be supplied to correct for any branch that is not completed at the center of the grid blocks.

Seg. Start #	Seg. End #	Branch #	Seg. Join #	X	Y
2	2	1	1	11	1
3	3	1	2	11	2
4	4	1	3	11	3
5	5	1	4	11	4
6	6	1	5	11	5
7	7	1	6	11	6
8	8	1	7	11	7
9	9	1	8	11	8
10	10	1	9	11	9
11	11	1	10	11	10
12	12	1	11	11	11
13	13	1	12	11	12
14	14	2	6	11	6
15	15	2	14	12	6
16	16	2	15	13	6
17	17	2	16	14	6
18	18	2	17	15	6
19	19	2	18	16	6
20	20	2	19	17	6
21	21	2	20	18	6
22	22	3	5	11	5
23	23	3	22	10	5
24	24	3	23	9	5
25	25	3	24	8	5
26	26	3	25	7	5
27	27	3	26	6	5
28	28	3	27	5	5
29	29	3	28	4	5
30	30	3	29	3	5
31	31	3	30	2	5

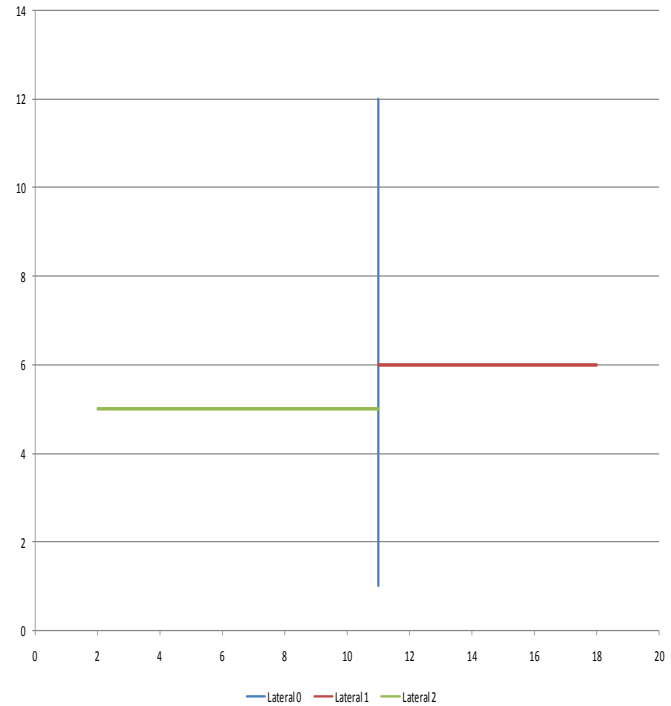


Figure 2-9: Structure of keyword WSEG with two laterals emanating from the motherbore

2.2.2. ICV Representation

Eclipse includes several keywords that can be used to restrict fluid flow. These keywords include WSEGVALVE, WSEGLABY, and WSEGFILM. All keywords apply the same restriction mechanism which is imposing additional friction pressure loss between the sand face and the tubing. The choice of the keyword depends on the physical means by which the restriction is achieved. For example, WSEGLABY imposes friction pressure by diverting fluid from the sand face to flow through a helical path of small channels. The friction pressure in this case is a function of the diameter of the flow channels and the length of the device. Although this keyword can achieve flow restriction, it is physically impossible to adjust the length of the device or the diameter of the flow channel periodically.

In this problem, WSEGVALVE keyword is chosen to represent ICVs. It represents a subcritical valve that imposes an additional pressure drop due to flow through a constriction with a specified area of cross section. The pressure drop across an ICV

is calculated using a homogeneous model of subcritical flow through a tube containing a constriction:

$$\delta P = \delta P_{cons} + \delta P_{fric} \quad (2.2)$$

where:

δP_{cons} accounts for pressure drop due to flow through constriction and is calculated by:

$$\delta P_{cons} = C_u \frac{\rho q_m^2}{2A_c^2 C_v^2} \quad (2.3)$$

where:

C_u is a unit conversion constant

ρ is the density of the fluid mixture

q_m is the volumetric rate of the fluid mixture

A_c is the cross-section area of the constriction

C_v is a dimensionless flow coefficient for the valve

δP_{fric} accounts for any additional pressure drop due to flow in the horizontal lateral. It is calculated using the standard expression for the homogeneous flow frictional pressure loss through a pipe:

$$\delta P_{fric} = 2C_u f \frac{L}{D} \rho q_m^2 A_p^2 \quad (2.4)$$

where:

f is the Fanning friction factor

L is the length of the tube in the horizontal lateral

D is the diameter of the pipe

A_p is the area of the tube

The pressure drop is a function of the friction pressure drop due to flow in the horizontal lateral and the friction pressure drop due to flow through an ICV. Since the friction pressure drop due to the horizontal lateral depends on the amount of fluid flowing through the lateral and therefore on the ICV configuration, the total pressure drop is a function of the ICV which is controlled by changing the cross section area of the ICV (A_c). The cross section area ranges between zero (ICV fully closed) and 0.022 ft² (ICV fully open). However, ICVs should be designed for each field separately as every field has different porosity and permeability and therefore different production rates.

An Eclipse include file, shown in Figure 2-10 is used to represent ICVs in this report. The fifth record which is the ICV area is continuously modified by MATLAB GA to change the ICVs settings.

```

File: valvecontrol.dat

WSEGVALV
  'WELL1' 7  0.686  0.00062  0 3* /
/
WSEGVALV
  'WELL1' 14  0.686  0.022  0 3* /
/
WSEGVALV
  'WELL1' 22  0.686  5e-005  0 3* /
/

```

Figure 2-10: Eclipse ICV file

2.3. ICV Design

Several production simulations should be carried out to design and optimize the ICV sizing. Production rates vary from one field to another and are function of the ICV size. In order to find the optimum ICV configuration that optimizes an objective function whether it is maximizing oil recovery, maximizing net present value or minimizing water production ICVs should be designed in such a way that each setting yields different production rate and therefore significantly impact the optimization process.

The ICV design process depends mostly on the production capability of each lateral. However, most oil companies generalize the design process and make it depend on the average field production rate rather than individual laterals production rates. The constant field design is better for logistic purposes such as maintenance and surveillance work. Since all the cases that will be shown in the subsequent chapters include only one well in each example field, ICV design will depend on the production rate from each individual lateral.

According to Equation 2.2, the total pressure drop (δP) is the sum of pressure drop due to fluid flow through the ICV (δP_{cons}) and the horizontal section (δP_{fric}). Pressure drop due to the ICV depends mostly on the area open to flow (A_c) and the magnitude of the production rate (q_m). Pressure drop in the horizontal section also depends on the production rate and Fanning friction factor (f) which indirectly depends on production rate through the Reynolds number. The variable production rate and the fact that the produced fluid is multiphase (multiphase flow creates different fluid regimes) result in different Fanning friction factor and therefore variable total pressure drop. The variable total pressure drop term indicates a nonlinear relationship between the ICV setting and the production rate.

For the purpose of this research, ICV size was chosen to best fit each optimization problem. ICV settings were discretized so each setting gave more or

less equal production rate even though sometimes that is impossible. Below are some considerations that have been made when designing the ICV:

- Simulation runs were performed to determine the maximum and minimum production rates for each lateral for two cases. These cases were when all laterals were producing together and when only one lateral was producing at a time.
- The area of an ICV was discretized based on the minimum and maximum production rate. The number of intermediate ICV settings is usually predefined by the manufacturing company.
- The minimum ICV setting corresponded to zero production rate while the maximum ICV setting corresponded to the maximum production rate.
- If production rate was significantly different from one lateral to another, ICVs with different sizes were applied although this might not be a feasible approach for all oil companies.
- The new ICV settings were tried out on the two cases; the case with all laterals producing, Figure 3-3, and the case with only one lateral producing at a time, Figure 3-2. If more than half of the ICV settings in a lateral gave the same production rate, this was taken to show that the maximum production rate should be reduced.

2.4. Optimization Framework

A flowchart of the overall optimization process is shown in Figure 2-11. The figure shows how MATLAB GA communicates with Eclipse to send and receive optimization parameters.

In step one, a population of binary strings is created. An individual is converted to the corresponding decimal string in step two. Then the decimal string is discretized to the desired number of ICVs settings. For example, a nine-bit binary string is converted to three-part decimal string which corresponds to three ICVs

settings. Since 99% of the optimization CPU time is spent in evaluating the objective function (i.e. the reservoir simulations), a library is created for each reservoir realization. The library contains any ICV setting that was proposed by the MATLAB GA and its corresponding objective function result (i.e. NPV). Before the ICVs settings are sent to the simulator, the optimization code checks the library for any identical ICVs settings ran earlier. If these settings are available, the simulator will not run and the CPU time will be saved. If the ICVs settings are not available, they will be written in a text file to be supplied to Eclipse. In step six, Eclipse is run with the supplied ICVs settings. Once the simulation run is finished, the MATLAB GA reads the simulated parameters, i.e. cumulative oil production and cumulative water production in this problem, and calculates the objective function. These steps are repeated for each individual in the population before the selection process takes place. At this time, the ICV setting and its corresponding objective function value will be stored in the library for future use. Once all individuals are simulated, the GA ranks these individuals based on their fitness function ratio and then selects the individuals that will contribute to the creation of the next generation. GA operators such as crossover, mutation, and elitism are applied to the selected individuals to form the next generation. The whole process is repeated for the next generations until termination criteria are met. The GA will be terminated if the specified generation number is reached or if there is no improvement in the objective function for 50 consecutive generations.

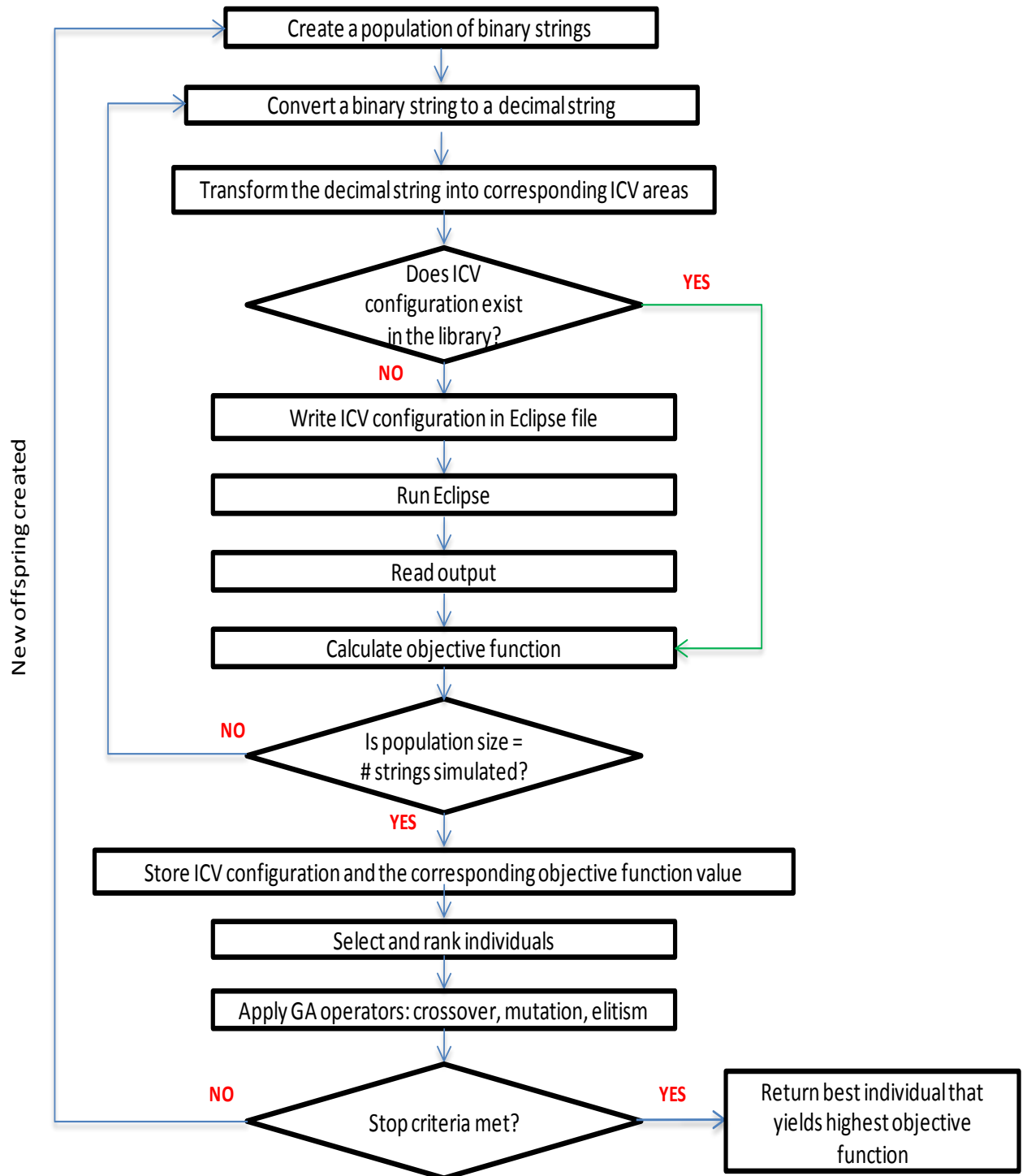


Figure 2-11: Flowchart of the optimization framework

CHAPTER 3

3. Applications on Various Reservoir Models

This chapter will present the applications of the optimization methodology to three different reservoir models. The complexity of the reservoir models increased from a simple synthetic model to dual porosity, highly fractured model. Thus, high impact GA parameters such as population size and generation number were chosen on a case-by-case basis to ensure optimum results are attained. In addition, ICVs sizes were determined for each case to ensure that each ICV setting can provide different production rate. Different objective functions such as recovery factor, net present value and water cut minimization were evaluated. The optimum ICV setting were determined using exhaustive search for all three cases to compare the true global solution to that obtained using the optimization method. This provided the opportunity to evaluate the effectiveness of the optimization methodology and the impact of various GA parameters.

3.1. Synthetic Model – Water Cut Minimization

3.1.1. The Synthetic Model

The synthetic model is a heterogeneous, isotropic, two dimensional, fluvial channel reservoir model. The reservoir dimensions are $2000 \times 2000 \times 50$ ft³ on a $40 \times 40 \times 1$ grid. Permeability values range from 0.45 md to 52 md and the distribution is given in Figure 3-1. Porosity was taken to be constant with a value of 0.3. Reservoir, rock, and fluid properties are given in Table 3-1 and Table 3-2. The reservoir is producing under five-spot pattern where a producer is placed at the middle of the reservoir (20×20) and four injectors are placed at the corners. The producer is a trilateral smart well where each lateral intersects 400 ft of the reservoir while the injectors are conventional vertical wells. Water is injected at a target rate of 300 STB/D in

each injection well with a maximum bottomhole pressure of 8000 psi. Production is specified to occur at a target oil rate of 300 STB/D with a minimum bottom hole pressure of 100 psi. A minimum oil production rate of 100 STB/D was imposed as an economic constraint. The simulation was run for 1200 days.

Table 3-1: Synthetic model - reservoir and rock properties

Reservoir and rock properties	
Reservoir size	2000×2000×50 ft ³
Oil thickness	50 ft
Porosity	0.3
$k_x = k_y = k_z$	100 md
Compressibility	$0.5 \times 10^{-5} \text{psi}^{-1}$ @ 14.7 psi
k_{rw}	0.029 @ $S_w = 0.2$
k_{ro}	0.0838 @ $S_w = 0.2$
P_{bub}	3824 psi
OWC	9000 ft

Table 3-2: Synthetic model - fluid properties

	Density (lb_m/ft³)	Viscosity (cp)
Oil	54	1.16@ 14.7 psi
Water	58	1 @ 14.7 psi

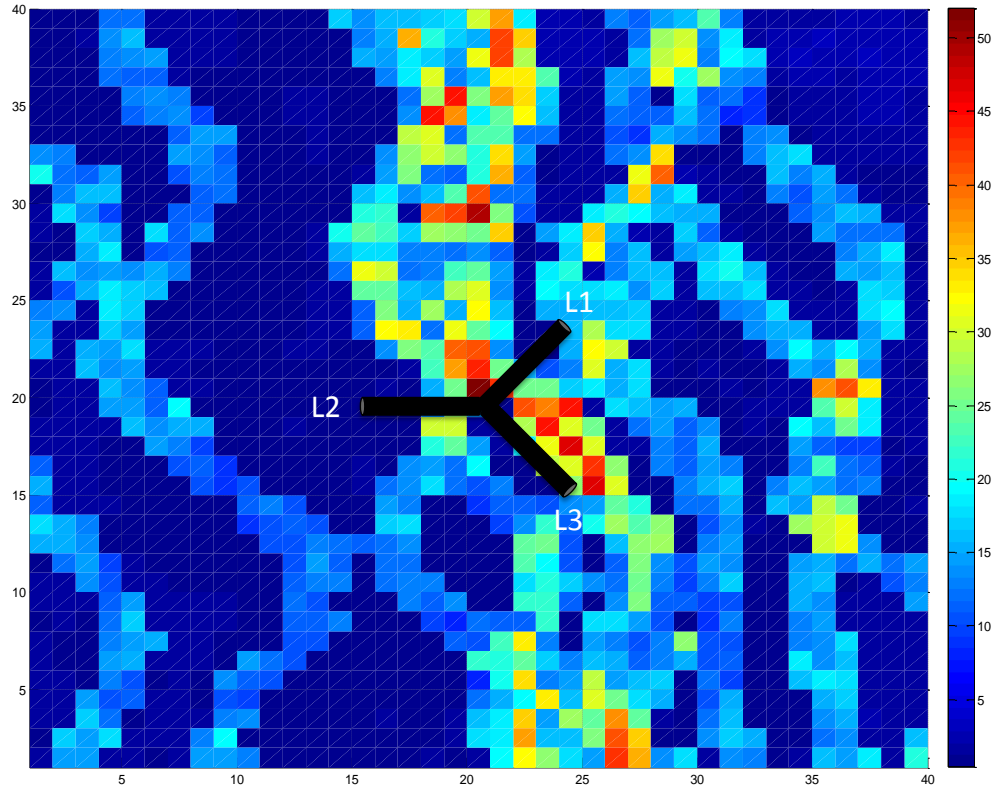


Figure 3-1: Synthetic model permeability distribution and producer location

Bottomhole pressure control strategy usually results in a large change in oil production during the first couple of years. For instance, oil production rate dropped by 40% in the first three years in this case. Since ICV settings were predetermined to be eight to match most ICVs used in the oil industry, the maximum ICV size was chosen based on the average oil production rate during the first three years rather than the maximum oil production rate, while the minimum ICV size was chosen to give zero oil production rate, Table 3-3. This ensures that each setting will produce more or less equal change in oil production.

Table 3-3: Areas corresponding to ICV settings for the synthetic models

Setting	Area (ft ³)
0	0
1	0.000038
2	0.00008
3	0.00013
4	0.00019
5	0.00027
6	0.00038
7	0.00057

On the other hand, individual lateral oil production rate is different when each lateral produces by itself from that when they all produce together. This difference is significant in the case of lateral two and therefore settings six and seven did not change the production rate, Figure 3-3.

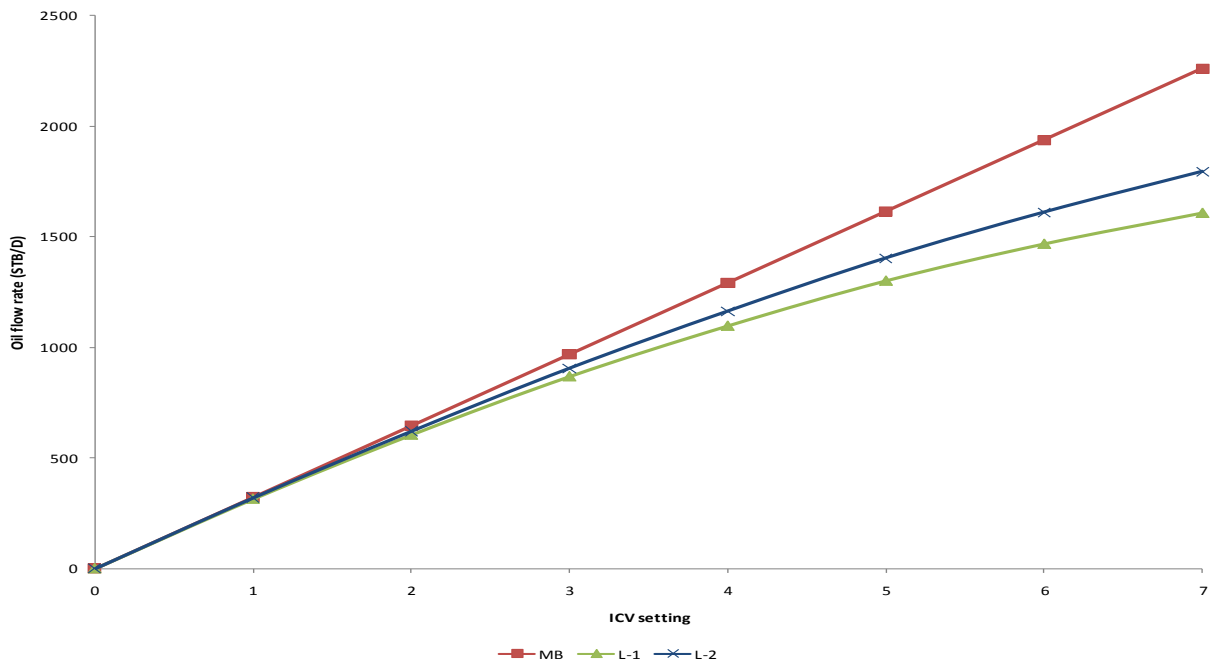


Figure 3-2: Oil flow rate vs. ICV setting when only one lateral is producing

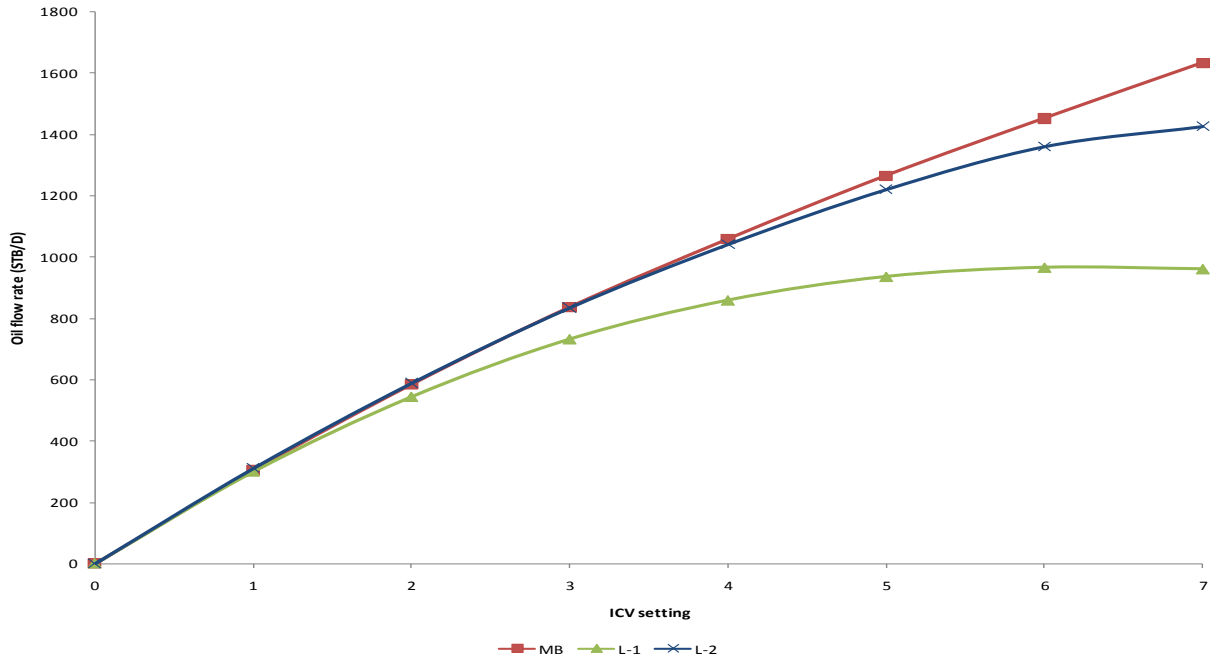


Figure 3-3: oil flow rate vs. ICV setting when all laterals are producing

3.1.2. Optimum ICV Setting – Water Cut Minimization

The objective was to find the optimum ICV configuration that yields the minimum water cut. Production and injection controls have been specified so that all possible ICV configurations are capable of producing 300 STB/D of oil for 1200 days. This will ensure fair and consistent comparison. Exhaustive search has been made to determine the global optimum ICV configuration. Knowing the global optimum ICV configuration provided the opportunity to evaluate the effectiveness of the optimization by comparing to the results of the exhaustive search. Also, the fact that water cut was determined at every possible ICV configuration allowed for intensive sensitivity analysis without the need to perform additional simulations.

Since all configurations are capable of achieving the production target, the optimized parameter (which is water cut) is affected by heterogeneity; i.e., permeability, and its influence on water front advancement. It was realized from the exhaustive search that the optimum ICV configuration is (0,7,0) meaning that both laterals one and three are closed while lateral two is fully open. In fact, any

ICV configuration that involves laterals one and three being closed will yield the minimum water cut. Figure 3-4 shows the effect of laterals one and three on the optimum solution, with lateral two being kept fully open. We can see how water cut increases as we open both laterals one and three.

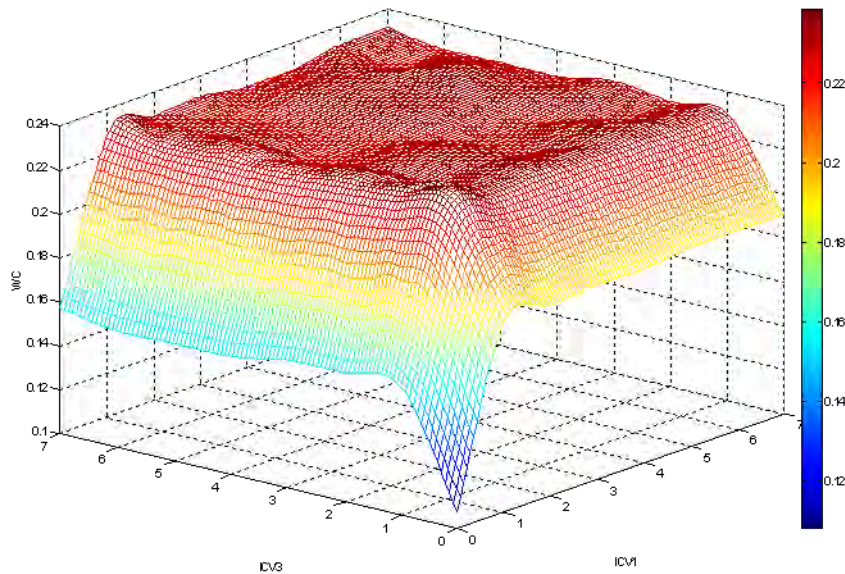


Figure 3-4: Solution surface with lateral two kept at fully open position

Analysis was carried out to test the GA optimization performance. As mentioned earlier, a population size of nine (which is equivalent to the solution string length) was used for ten generations. Figure 3-5 shows the progress of the optimization run in terms of the average value of the fitness function, water cut in this case, and the best individual. It is worth noting that the average water cut decreased drastically in the early stages until it became equal to the best individual at the end of the optimization run. In addition, the value of the best individual reached the global optimum solution which is at $WC = 10.81\%$ on the third generation. This is a clear indication that GA optimization is suitable for the problems of this type due to the fast rate of convergence.

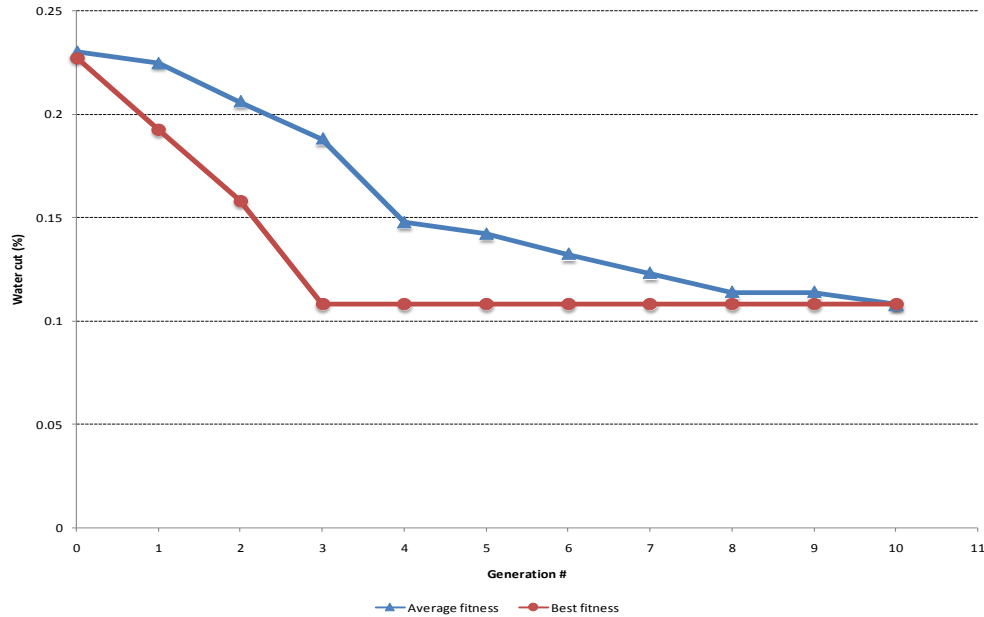


Figure 3-5: Progress of GA optimization for the Synthetic model

3.2. Offshore Model – Net Present Value Maximization

3.2.1. The Offshore Model

The offshore model represents a giant sandstone field located in the Middle East. Figure 3-6 shows grid structure and initial water saturation. The model has 23×41×14 irregular grid blocks. Grid block sizes range from 28,800,000 ft³ to 230,400,000 ft³. Larger grid blocks are located on the sides of the model where production wells will not usually be drilled. Rock and fluid properties are shown in Table 3-4 and Table 3-5.

Water Saturation

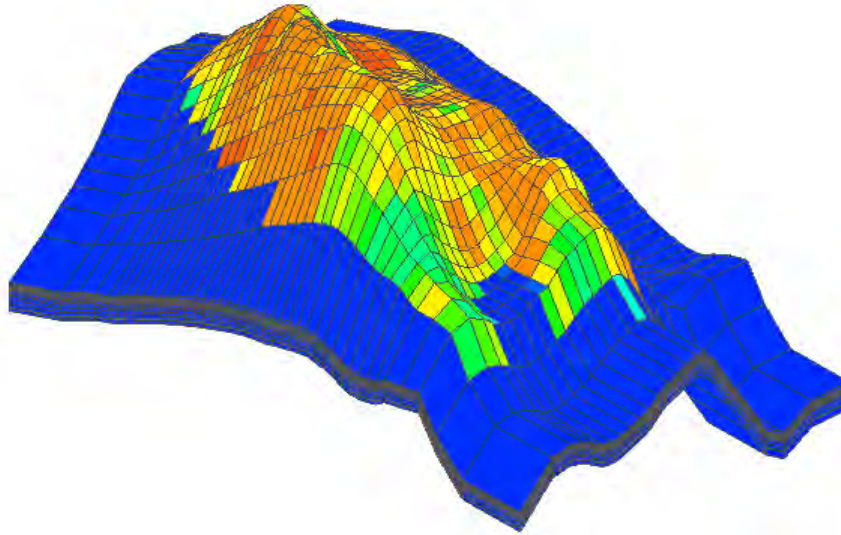
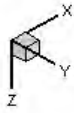


Figure 3-6: Offshore model 3D grid structure and initial water saturation

Table 3-4: Offshore model - reservoir and rock properties

Reservoir and rock properties	
model size	23×41×14 grid blocks
Oil thickness	136 ft
Porosity	0.23
Average permeability	300 md
k_v/k_h ratio	0.05
Compressibility	$6.8 \times 10^{-6} \text{psi}^{-1}$ @ 300 psi
k_{rw}	0.05 @ $S_w = 0.57$
k_{ro}	0.04 @ $S_w = 0.57$
k_{rg}	0.054 @ $S_g = 0.53$
Original reservoir pressure	2316 psi @ 4370 ft SS
P_{bub}	876 psi
OWC	5052 ft SS

Table 3-5: Offshore model – fluid properties

	Density (lb_m/ft³)	Viscosity (cp)	FVF (V/V)
Gas	46.80	0.0205 @ 3000 psi	0.8790 @ 3000 psi
Oil	55.36	2.58 @ 3000 psi	1.4361 @ 3000 psi
Water	72.38	1 @ 3000 psi	1.003 @ 3000 psi

The field is currently undeveloped. So, a smart well is placed as a proof of concept to test and evaluate the technology on reservoir, well performance, and overall reservoir management strategies. The reservoir is producing under primary recovery and the production well is placed downdip to ensure water production toward the end of the simulation run. The production well is a trilateral smart well where each lateral intersects approximately 10,000 ft of the ninth layer of the reservoir. Figure 3-7 shows the permeability map of layer nine. Production is specified to occur at a target oil rate of 4,000 STB/D with a minimum bottom hole pressure of 1000 psi. A minimum oil production rate of 100 STB/D was imposed as an economic constraint. In addition, a maximum water production of 400 STB/D was imposed. The simulation was run for 10 years.

Production control strategy was used in the simulator specification to ensure a constant oil rate of 4,000 STB/D is produced. Although individual laterals might not produce the target rate, ICVs were designed to ensure a combined target rate of 4,000 STB/D. ICV settings and the corresponding areas are given in Table 3-6.

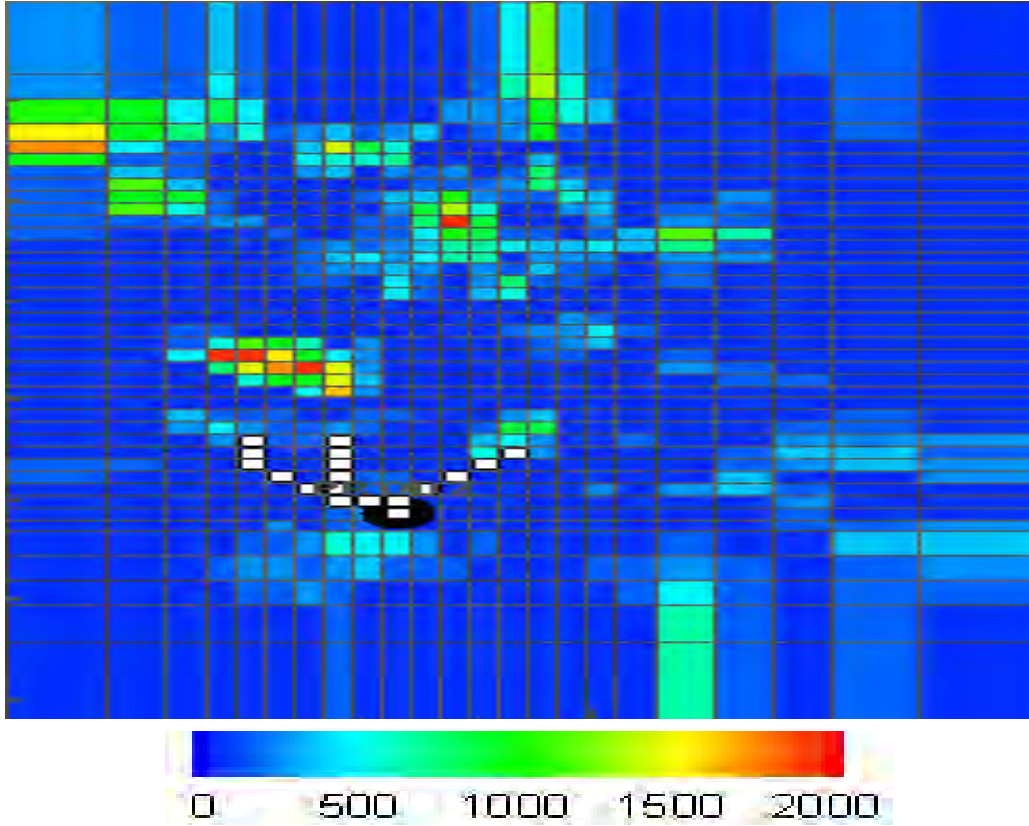


Figure 3-7: Offshore model - permeability distribution of layer nine

Table 3-6: Areas corresponding to ICV settings for the offshore models

Setting	Area (ft ³)
0	0
1	0.00006
2	0.00021
3	0.00026
4	0.00041
5	0.00065
6	0.0011
7	0.0080

3.2.2. Optimum ICV Setting – NPV Maximization

The objective in this case was to find the optimum ICV configuration that yields the maximum net present value (NPV). The production well was specified to produce at a controlled rate of 4,000 STB/D even though some ICV configurations might not be able to. In addition, the production well was allowed a maximum water production of 400 STB/D. This increased the weight of water production in the objective function and avoided the trivial optimum fully open ICV configuration (7,7,7). NPV was calculated with a net oil profit of \$50/bbl and water handling cost of \$20/bbl.

This case was first simulated with the trivial ICV configuration of (7,7,7) which comprises the base case. Figure 3-8 shows the production well rate and the corresponding water cut. The production rate was initially 1600 STB/D and the decline was very shallow. The shallow decline in production rate indicates that the production well is capable of producing the target rate of 4,000 STB/D. However, the production well is restricted to maintain the target water production limit of 400 STB/D. Figure 3-10 shows that lateral-0 (MB) was the main source for water production. So, intuitively restricting lateral-0 will boost the cumulative production up although lateral-0 produces high oil rate.

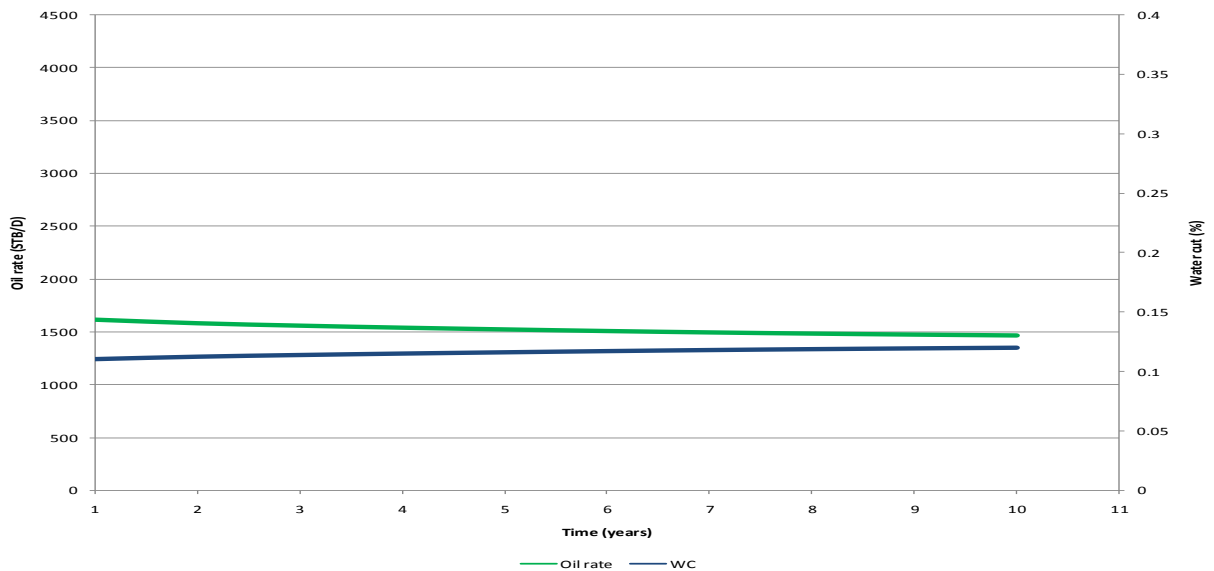


Figure 3-8: Offshore model - production rate and water cut (base case)

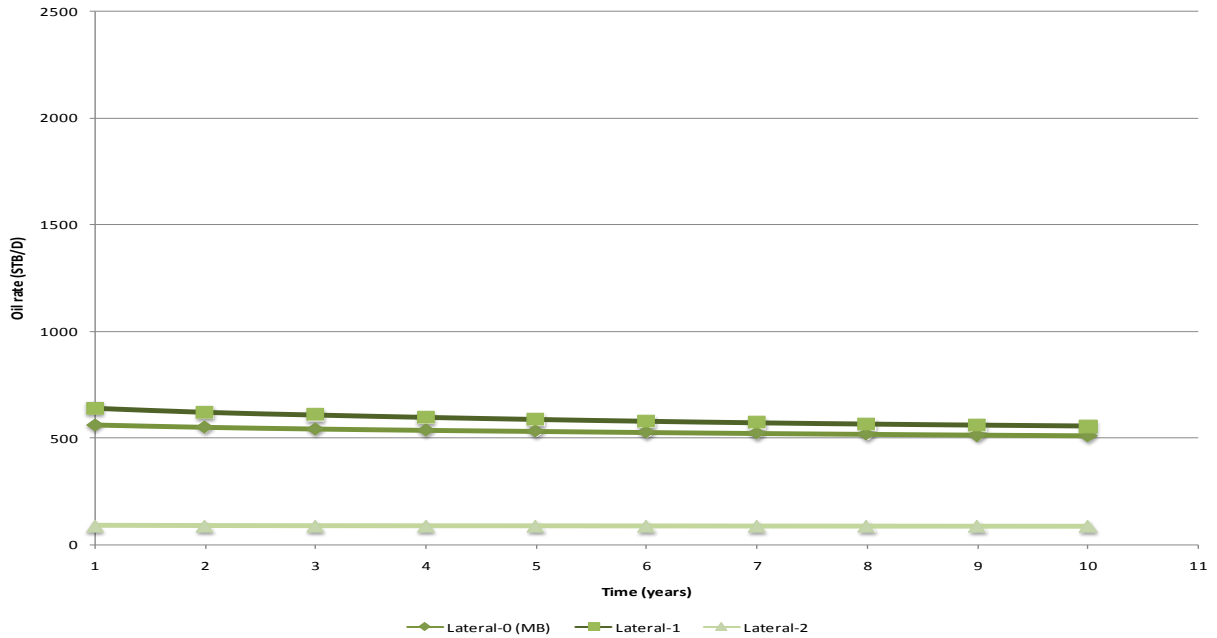


Figure 3-9: Offshore model - individual lateral production rate (base case)

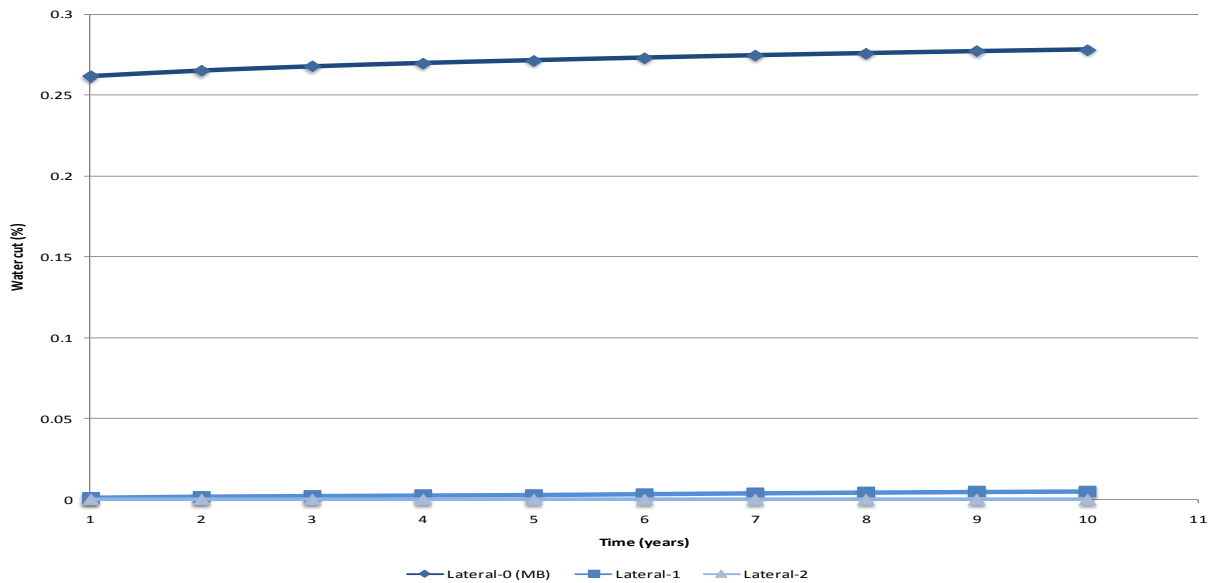


Figure 3-10: Offshore model - individual lateral water cut (base case)

Exhaustive search indicated that the optimum ICV configuration is (0,4,7). Although it was a high producing lateral, lateral-0 was fully closed to minimize water production and release the overall restriction on the well. It has been seen previously that lateral-0 was the main source of water. Lateral-2 was fully open because lateral-2 is already a low producing lateral with no water production. So, it

makes a perfect sense to produce as much as possible from lateral-2 since it does not add any water production. With lateral-0 closed, lateral-1 has to be open to a certain degree to compensate the loss in oil production. We can see that lateral-1 is adjusted at setting four which balances oil production and water production. Figure 3-11 shows the effect of lateral-1 and lateral-2 on NPV. NPV drops when ICV2 is greater than four.

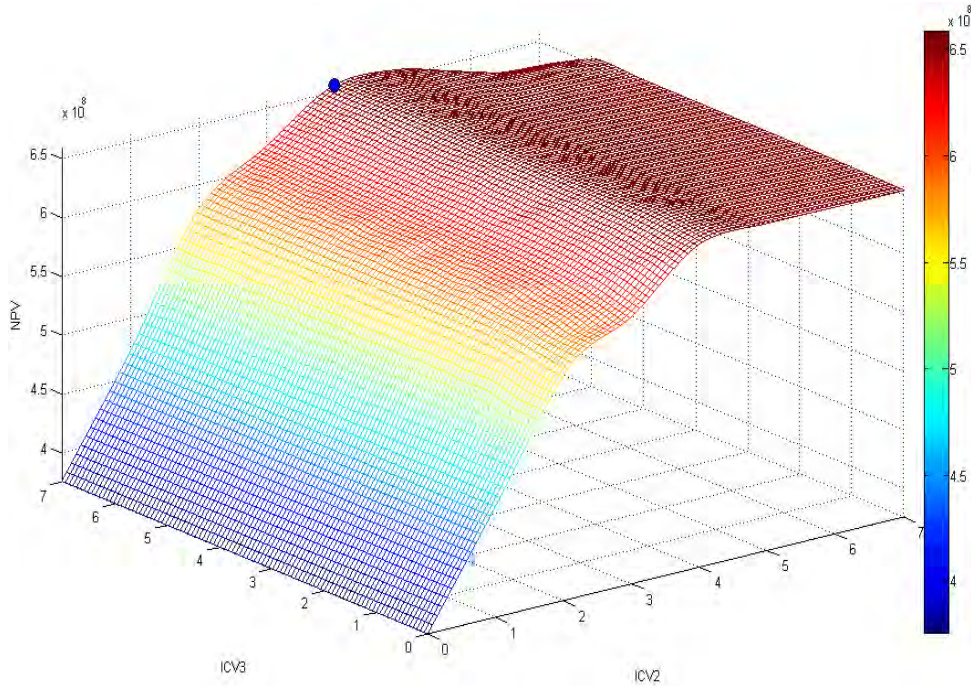


Figure 3-11: Solution surface with lateral-0 (MB) fully closed

Analysis was carried out to test the GA optimization performance. Similar to the synthetic case, a population size of nine was used for twenty generations. Figure 3-12 shows the progress of the optimization run in terms of the average value of the fitness function, NPV in this case, and the best individual. The average NPV is noted to increase rapidly during the first five generations. In addition, the value of the best individual reached the global optimum solution which is at NPV = 654.5 MM\$ on the fifth generation. This indicates that a population size that is equivalent to the solution string length and a generation number of five was adequate for this case.

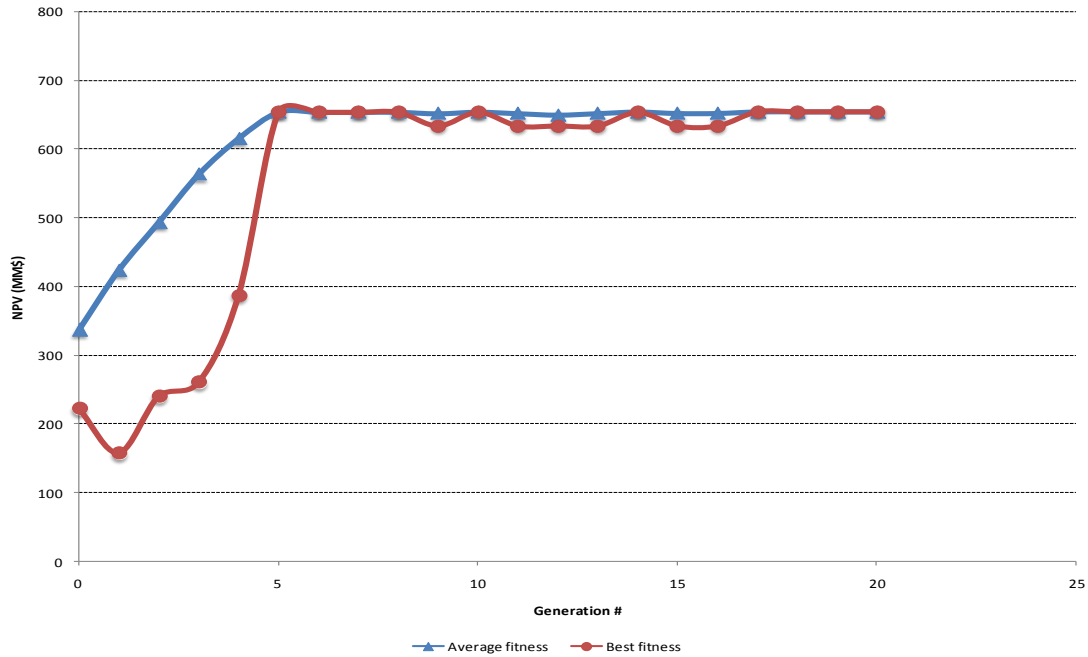


Figure 3-12: Progress of GA optimization for the offshore model

Figure 3-13 and Figure 3-14 show the cumulative and individual lateral oil production rates. We can see in the optimized case that the production well is now able to maintain the target rate of 4,000 STB/D throughout the simulation run time with minimum water production. In addition, lateral-0 (MB) which was the main source of water is closed completely. The loss in oil production was compensated by moderately producing from lateral-1.

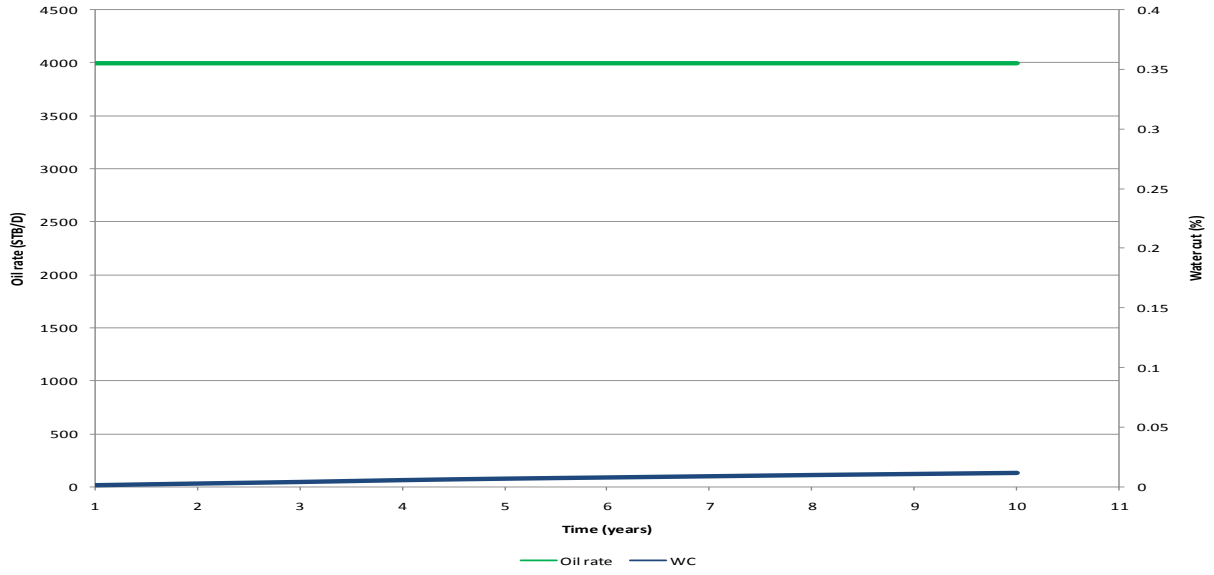


Figure 3-13: Offshore model - production rate and water cut (optimized case)

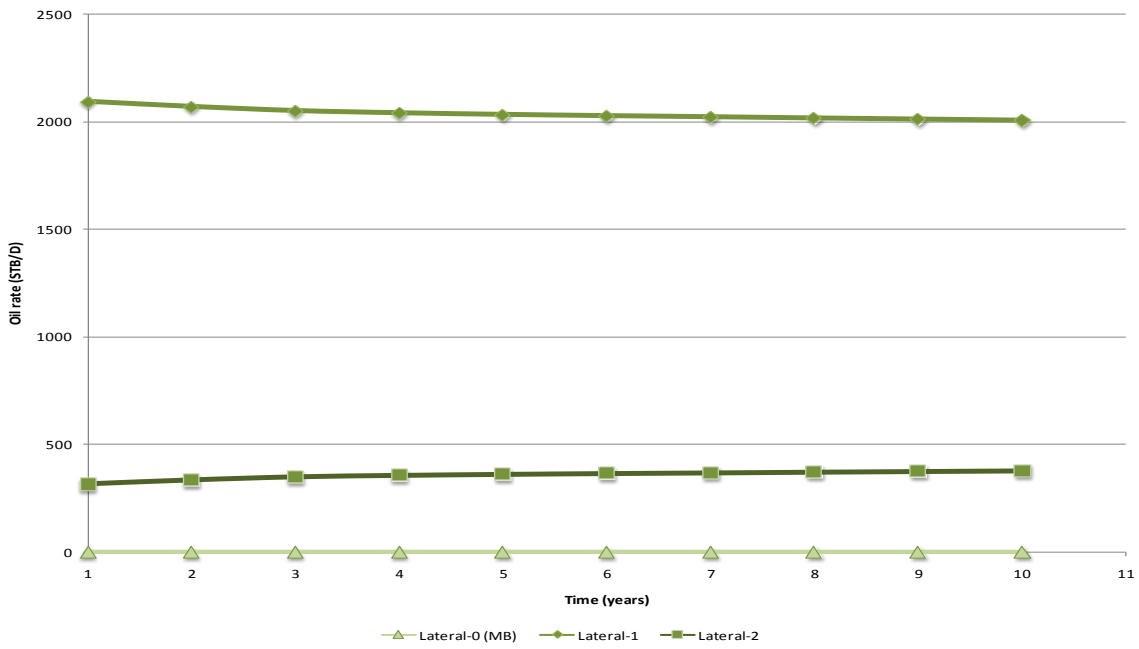


Figure 3-14: Offshore model - individual lateral production rate (optimized case)

3.3. Onshore Model – Production Plateau

3.3.1. The Onshore Model

The onshore model represents a sector model of an onshore field located in the Middle East. The field is a giant anticline trap that produces from two main reservoirs. These reservoirs are an upper and lower carbonate reservoirs separated by a thick non-reservoir formation. The upper reservoir is prolific throughout the entire field with an average vertical permeability of 400 md while the lower reservoir has an average vertical permeability of 1-2 md only. Although these reservoirs are separated by a thick non-reservoir layer, production data suggests that vertical communication between the two reservoirs exists and is believed to be caused by fractures that cut through the non-permeable layer. The onshore model contains $51 \times 19 \times 26$ square grid blocks. It focuses only on the top reservoir which is divided into 26 layers. Figure 3-15 shows the grid structure and initial water saturation. Rock and fluid properties are available in Table 3-7 and

Table 3-8. The simulation was run for 20 years.

Water Saturation

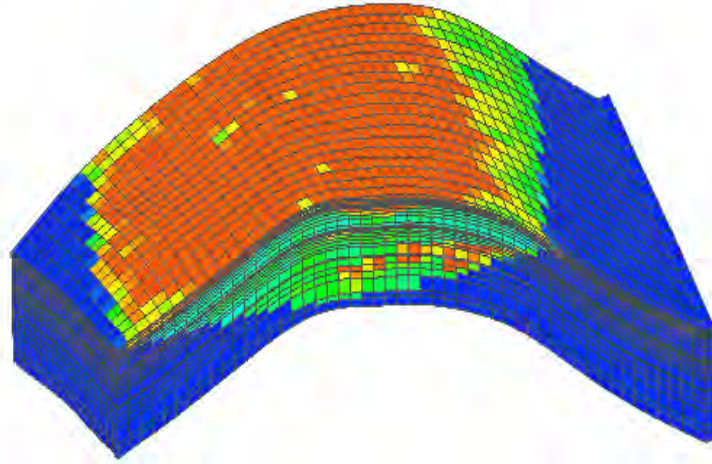
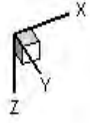


Figure 3-15: Onshore model 3D grid structure and initial water saturation

Table 3-7: Onshore model - reservoir and rock properties

Reservoir and rock properties	
model size	12,750×4,750×6,500 m ³
Porosity	0.16
k _x	546 mD
k _y	401 mD
k _z	11.6 mD
Compressibility	2.0×10 ⁻⁶ psi ⁻¹ @ 3410 psi
k _{rw}	0.32 @ S _w = 0.54
k _{ro}	0.005 @ S _w = 0.54
k _{rg}	0.067 @ S _g = 0.54
Initial reservoir pressure	3524.9 psi
Initial water saturation	0.712
P _{bub}	2533.5 psi

Table 3-8: Onshore model – fluid properties

	Density (lb_m/ft³)	Viscosity (cp)	FVF (V/V)
Gas	0.06095 @ 14.7 psi	0.0112 @ 14.7 psi	0.84 @ 3330 psi
Oil	52.36 @ 14.7 psi	1.34 @ 14.7 psi	1.0764 @ 14.7 psi
Water	71.85 @ 14.7 psi	1 @ 14.7 psi	1.0207 @ 3400 psi

The field is very mature and producing under secondary recovery. The production well was drilled as a trilateral smart well in the west side of the model sector (I = 15, J = 12) in the first layer. Laterals two and three are close to vertical fractures network suggested by loss of circulation while drilling. The production well properties are given in Table 3-9. Production was specified to occur at a target oil rate of 3,000 STB/D with a minimum bottom hole pressure of 1800 psi. A minimum oil production rate of 100 STB/D was imposed as an economic constraint. A five-spot injection scheme that consists of four power water injection wells (PWI) injected water at a constant rate of 20,000 STB/D (5000 STB/D/Well) in layers 3 through 26 allowing bottom-up sweep behavior. These four wells are located at the corners of the sector, Figure 3-16 . ICVs were designed to handle the target production rate of 3,000 STB/D. The ICV settings and the corresponding areas are given in

Table 3-10.

Table 3-9: Onshore model - production well properties

Lateral #	No. of segments	Length	Avg. effective kh
Lateral-0 (MB)	5	6,179'	12,453
Lateral-1	6	4,086'	12,221
Lateral-2	8	4,333'	12,256

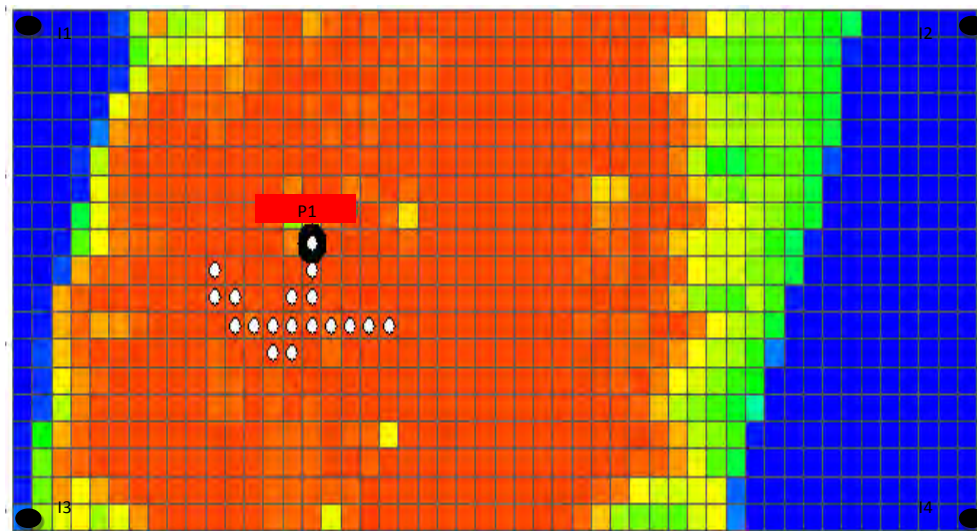


Figure 3-16: Onshore model – five-spot pattern on saturation map

Table 3-10: Areas corresponding to ICV settings for the onshore model

Setting	Area (ft ³)
0	0
1	0.00005
2	0.00015
3	0.00025
4	0.00039
5	0.00062
6	0.0015
7	0.01

3.3.2. Optimum ICV Setting – Production Plateau

The objective in this case was to find the optimum ICV configuration that prolongs the life of the well and extends the production plateau. Production plateau is defined as the time during which the well can produce at the constant specified production rate (3000 STB/D). Production plateau duration is important when increasing the recovery factor is a key issue, which is the case for most of National Oil Companies. Production plateau is extended by ensuring that the production well will produce dry oil (no water production) for longer period of time. Well rate control is used to ensure that the well will not exceed the target production rate no matter what the ICV configuration is.

A base case was defined to which the optimization result is benchmarked. The base case reflects the result that would have been achieved when producing the well at the current ICV configuration, which is (7,4,4). Notice that laterals two and three have been already restricted as a precautionary measure to mitigate water production from nearby fractures. Figure 3-17 shows the base case production oil and water rates. We can see that the production plateau duration is approximately four years. Two humps in oil rate are noticed in Figure 3-18 due to flow through nearby fractures that are close to laterals two and three.

Using the recommended population size of nine individuals, the optimization run resulted in adjusting the ICV configuration to (4,6,0). This adjustment extends the production plateau two additional years resulting in a total of six years of dry oil production, Figure 3-19. Figure 3-20 shows a slower drop in oil rate after water breakthrough as opposed to a faster drop in oil rate in the base case. This is due to the effect of fractures close to lateral three that accelerate water production, which was overcome by closing the ICV corresponding to lateral three.

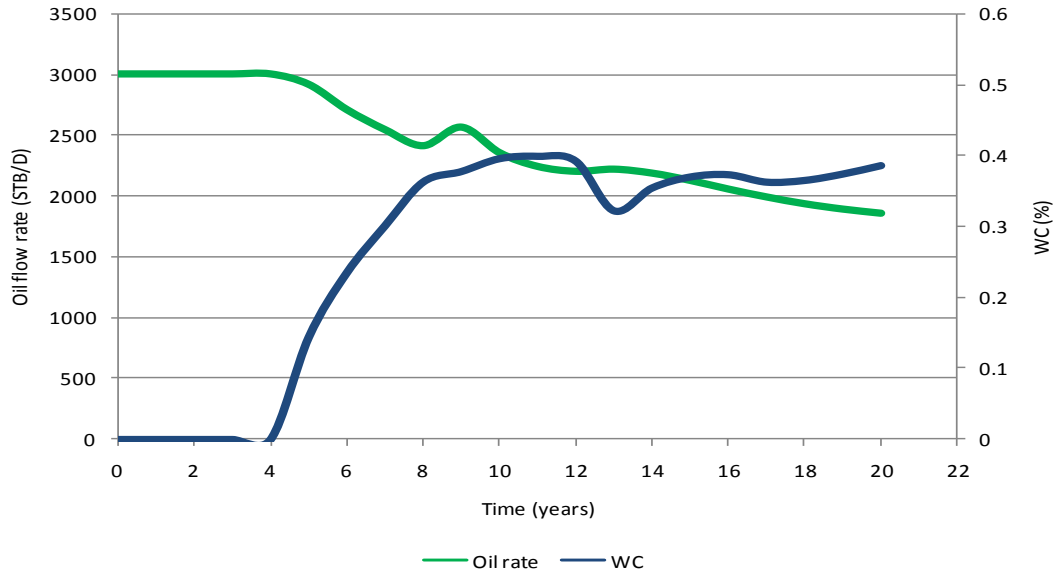


Figure 3-17: Onshore model – production rate and water cut (base case)

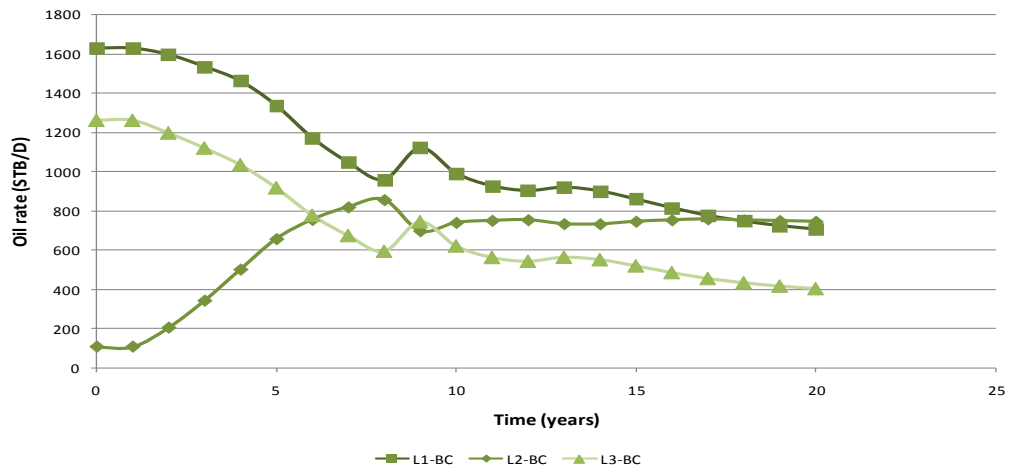


Figure 3-18: Onshore model - individual lateral production rate (base case)

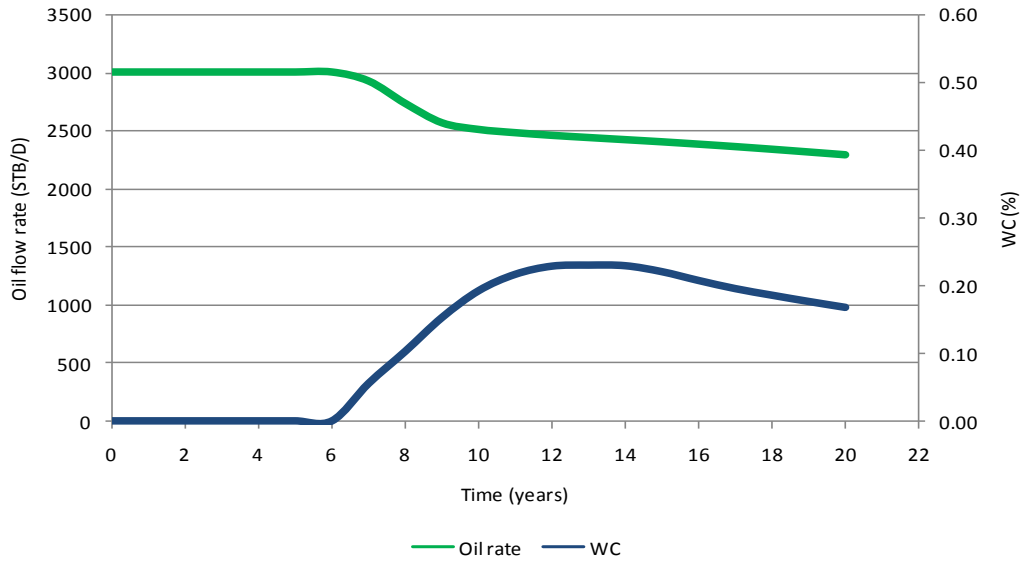


Figure 3-19: Onshore model – production rate and water cut (optimized case)

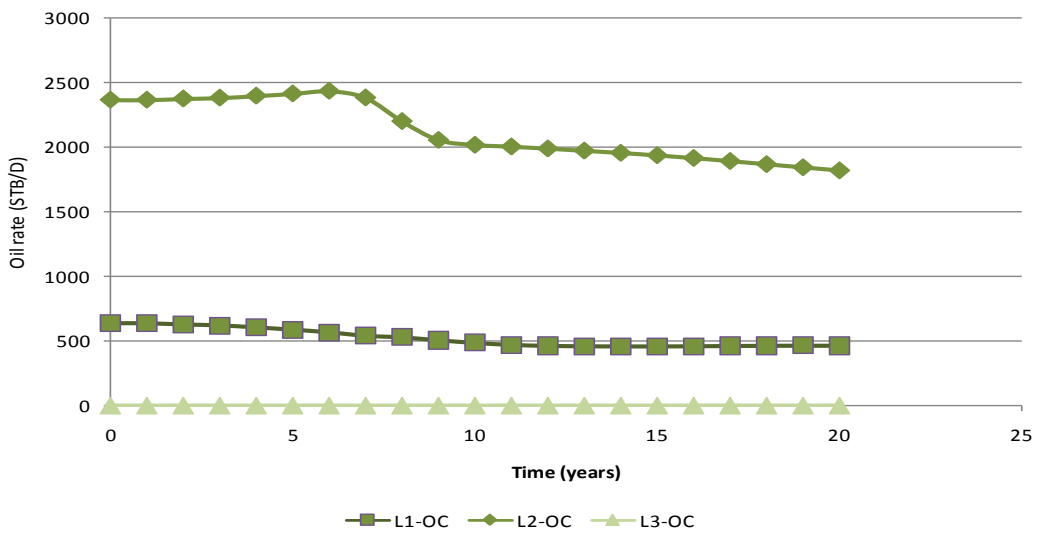


Figure 3-20: Onshore model - individual lateral production rate (optimized case)

CHAPTER 4

4. Fractures Effects on Smart Wells Optimization

A great portion of the world's hydrocarbon exists in naturally fractured reservoirs (Aguilera, 1995). One example is the largest oil field in the world, the Ghawar field, which poses a great challenge in terms of fracture complexity. Fractures display complicated flow behavior due to the extreme difference in permeability and porosity between the rock matrix and the fracture itself. Fractures have much greater permeability than the formation they penetrate. A fracture acts as a conduit or a 'highway' in the rock that transmits oil and gas which affects the flow behavior of the porous medium. However, fractures are associated with very low fluid storativity compared to the rock matrix (Horne 1995, p.36-41). This means that fractures do not store as much oil and gas as the matrix they reside in.

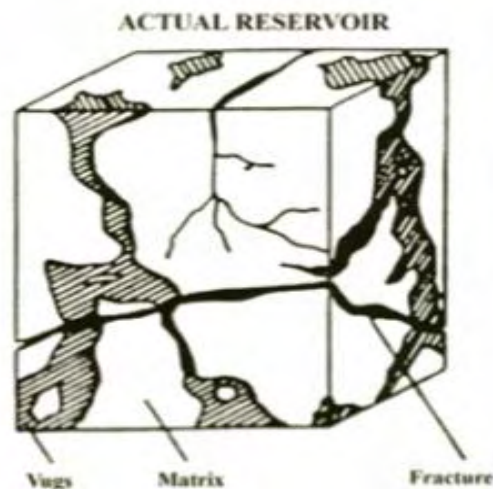


Figure 4-1: Fractures and matrix in reservoir (Warren and Root, 1963)

Fractures can be favorable or unfavorable in terms of hydrocarbon production (Mavco et al., 1998). For example, hydraulically induced fractures are introduced in tight gas reservoirs to enhance the low permeability matrix. On the other hand, fractures may cause water flooding projects to fail due to injected water being transmitted from injection wells to production wells through fractures leaving large amounts of bypassed hydrocarbon. This causes premature abandonment of production wells because of the inability to mitigate the high water production. A perfect example is the onshore model case discussed in Chapter 3. It has been seen how restricting production from lateral three which is close to the fracture allowed the production well to maintain its target and resulted in prolonging the well's life.

Fractures can be identified directly using cores, formation imaging logs, and drill cuttings. Figure 4-2 illustrates a formation imaging log that shows fracture spacing, formation orientation, and dip. Fractures can also be identified indirectly by loss of circulation while drilling, very high production in thin zones on production logs, and using well test analysis. Direct sources of fracture identification require the fracture to actually intersect the wellbore. Due to the huge difference in size between the wellbore and the reservoir, the percentage of fractures identified using direct sources is very small. Indirect sources of fracture identification on the other hand do not require the wellbore to intersect the fracture. In fact, indirect sources do not specify the location of the fracture as they only indicate the effect, i.e. earlier water breakthrough, loss of circulation, and high producing thin zone.

Since the chance that a well will intersect a fracture is slim, the exact location of a fracture is usually unknown. However, this can be compensated by approximating the location of the fracture in the reservoir model based on indirect sources of information at first and performing a series of simulation runs to history match the effect or anomalies caused by the fracture, i.e., water cut. Although history matching yields acceptable results, it is computationally expensive as it requires a large number of parameters to be adjusted. So, this chapter will discuss a

technique to investigate whether it is essential to know the exact location of the fracture to properly optimize the production from a smart well.

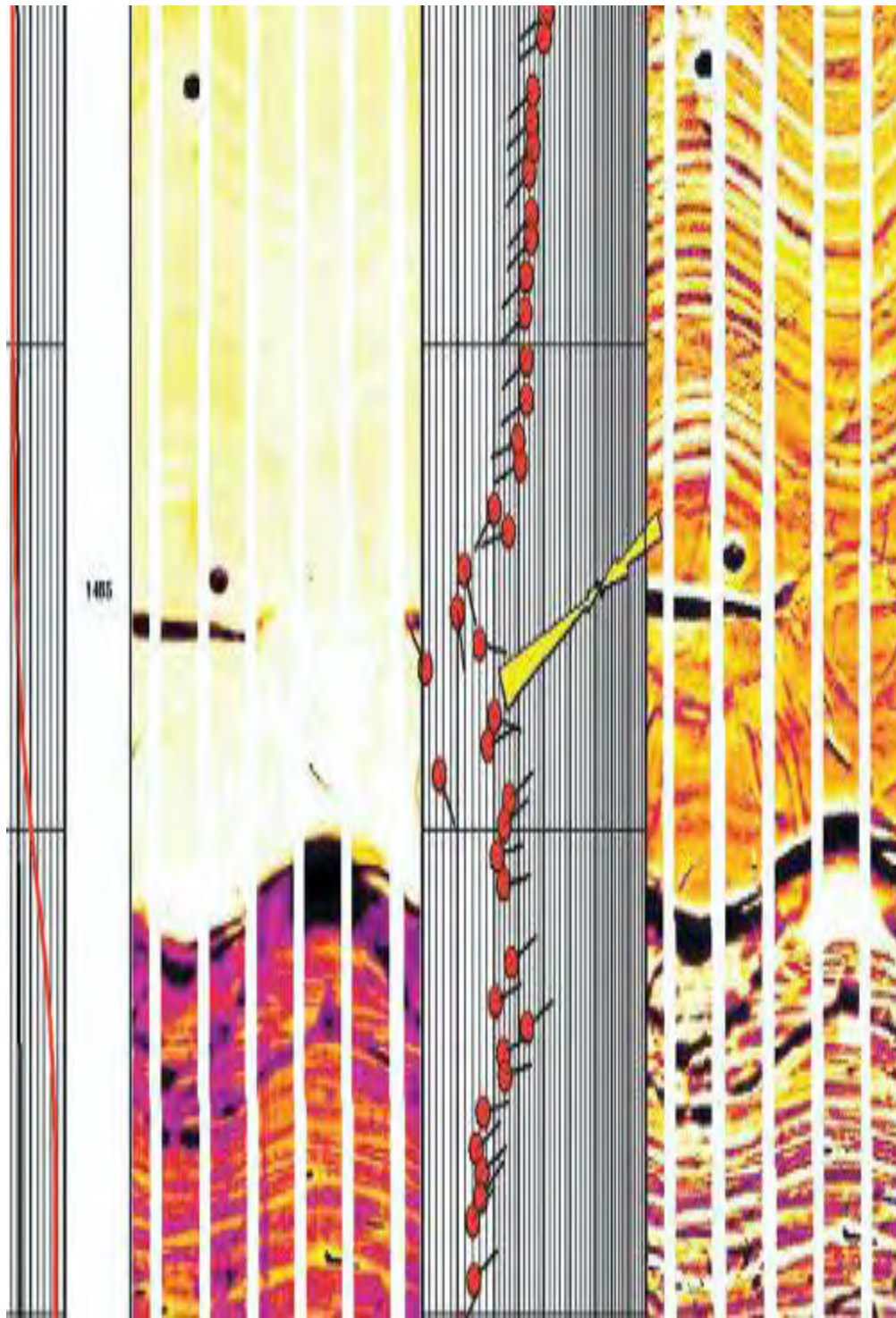


Figure 4-2: Fracture imaging log showing fracture spacing, formation orientation, and dip

4.1. Fracture Representation

Several techniques have been introduced in the literature to model fractured reservoirs. One technique used to model fractures is called Discrete Fracture Network (DFN). DFN is usually used when matrix has very low porosity and permeability. However, it can be extended to handle high porosity and permeability reservoirs where the concept of an effective matrix is introduced. In this research, a fairly new and simple technique called source model will be used as a DFN flow model. The technique was developed by Voelker in 2004. Source model is simply a shut-in ‘well’ that is not produced at the surface. However, the well is open to backflow between the source connections (grid blocks intersecting the source) instead, Figure 4-3. Technically, source model is represented as a group of connection transmissibilities constrained by a zero flow rate and hydrostatic equilibrium:

$$S^\alpha = \{T_1^\alpha, T_2^\alpha, \dots, T_j^\alpha; \rho_{fluid}; q = 0\} \quad (4.1)$$

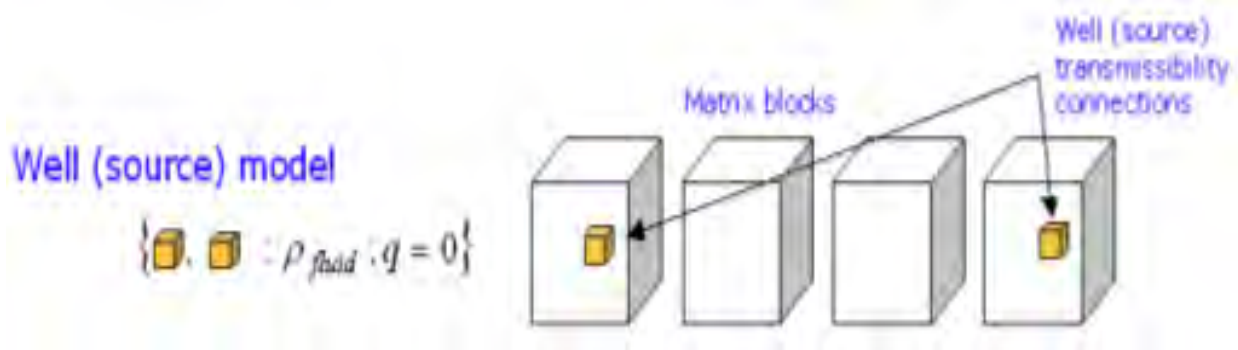


Figure 4-3: Source model technique as discrete fracture (Voelker, 2004)

In this research, the transmissibilities of connections are similar to the transmissibilities of the grid block hosting them since the fractures in this study are artificial and did not require history matching. Source model can be implemented in all conventional flow simulators. Advantages of using source model include:

- simplicity of implementation: adding DFNs is similar to adding wells and therefore can be used in multiple realizations.
- no alteration of flow simulator grid blocks.
- ability to use in mixed fracture system (small scale and large scale fractures).
- capability to use sources along a curve, Figure 4-4.

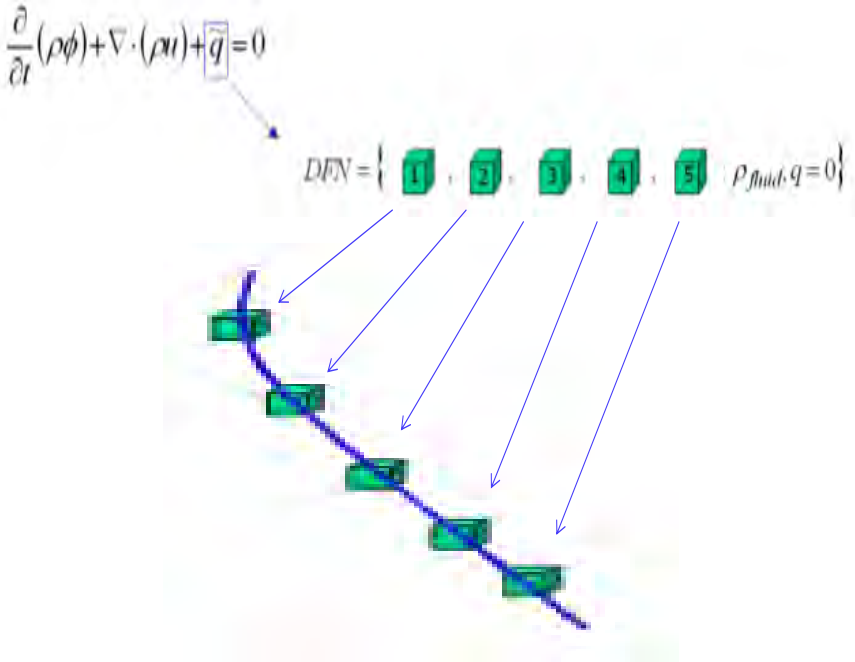


Figure 4-4: Source model representation as a curved fracture (Voelker, 2004)

4.2. Fracture Location Study

In order to investigate the sensitivity of the location of fractures on the optimization of a smart well, multiple realizations have been made. The fracture location in each realization was different. For a fair comparison between the case where we knew the fracture location and the case we did not, fractures were placed in the form of a rectangle that surrounded the actual location of a fracture, Figure 4-5. Although the exact location of a fracture might have not been known, it could be approximated using indirect sources.

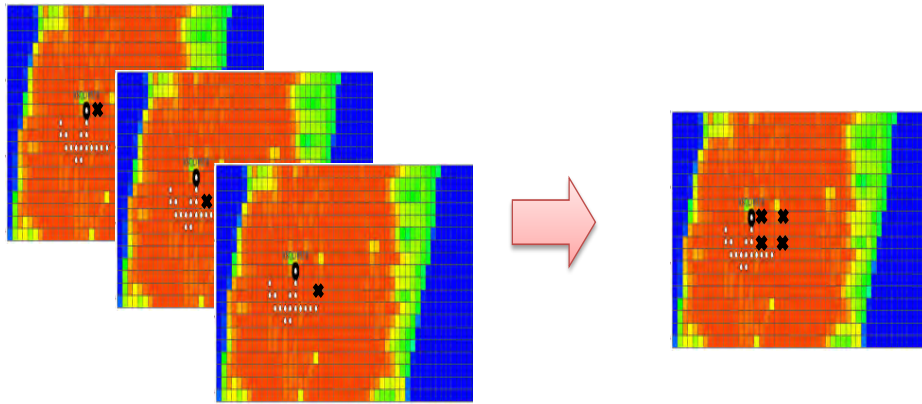


Figure 4-5: Multiple realizations comprising an area of possible fracture location

The expected value of the objective function of the multiple realizations was used for evaluation of fitness during the optimization.

$$E(obj\ fn) = \frac{obj\ fun_1^\alpha + obj\ fun_2^\alpha + \dots + obj\ fun_j^\alpha}{number\ of\ realizations} \quad (4.2)$$

where α is the case name, and j is the realization number.

The expected value of the objective function was compared against the value of the objective function of the realization with the exact location.

4.3. Fracture Location Study Framework

A flowchart of the fracture location study is given in Figure 4-6. In short, each candidate ICV configuration proposed by the GA was simulated on all reservoir realizations. The expected value of the objective function was calculated using the objective function values of all realizations. The expected value was used for evaluation and progress from one generation to the next. A library, similar to the one discussed in Chapter 2, was created for each case to minimize the time required to complete the run.

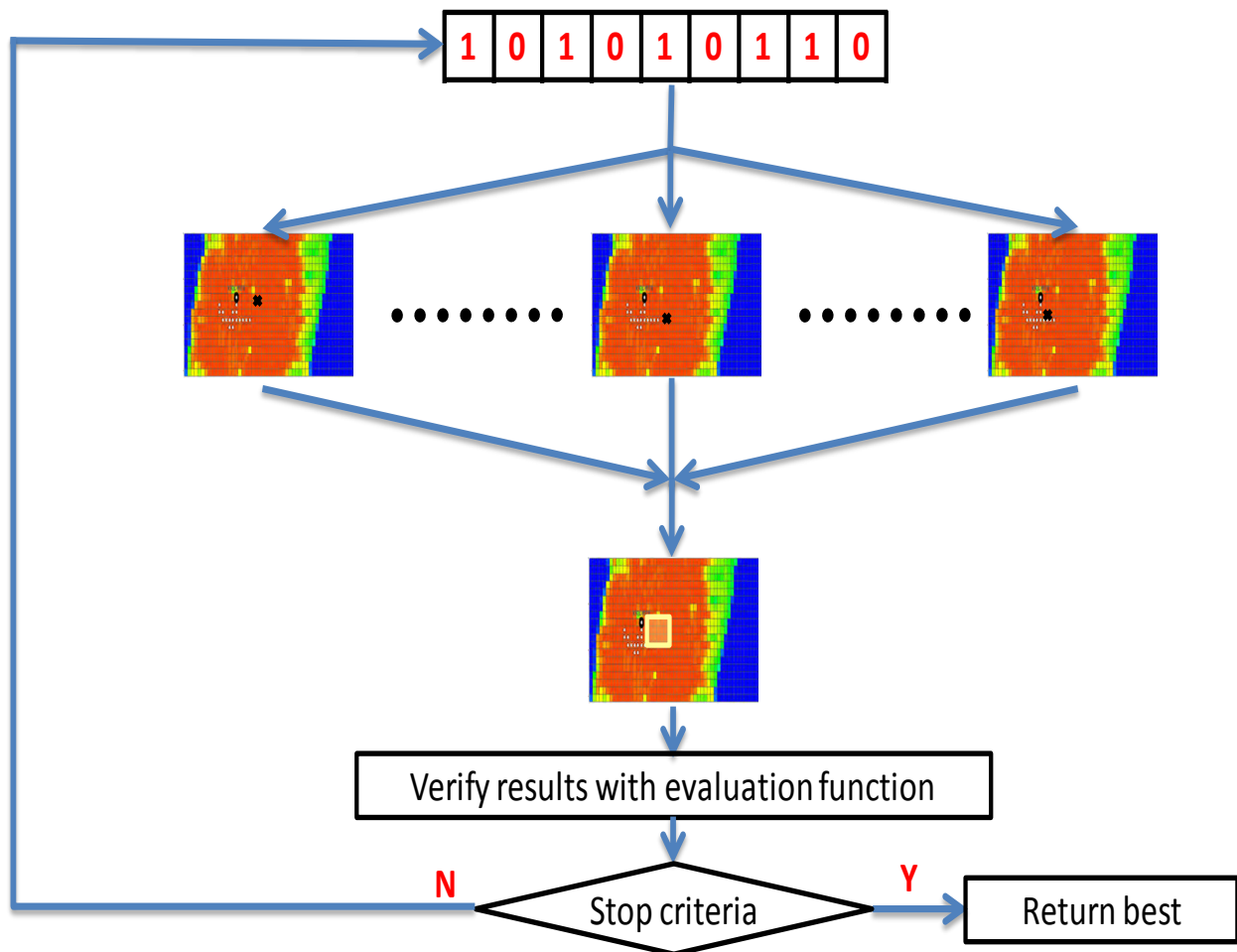


Figure 4-6: Framework of fracture location study

4.4. Onshore Model Fracture Study – Case One

As previously mentioned in Section 3.3.1, the onshore model represents a sector model of a giant field located in the Middle East. The main producing reservoir undergoes peripheral waterflood where water injection wells are placed on the flanks of the field. Since the sector model is approximately at the middle of the field, the waterflood is compensated by fluxes of oil and water coming from the four sides of the sector model. The reservoir is heterogeneous, isotropic, and naturally fractured. Although the reservoir sweep tendency in general is a bottom-up sweep, DFNs significantly affect specific well performance as water breaks through earlier in thin intervals. In fact, this phenomenon necessitates the use of Smart completion and production equalizers as production wells tend to die prematurely due to high water cut.

The source model approach was used to introduce DFN in two cases. These cases are Case 1a and Case 1b. Fractures were placed around the actual fracture comprising a square of 750 m × 750 m, Figure 4-7. The expected NPV which was the comparison criterion was an average of the NPVs resulted from all fracture realizations. Since fractures closer to the well normally result in lower NPV while fractures far away result in higher NPV, the expected NPV is more or less equivalent for any fracture at similar distance, as is the case for the fracture realizations shown in Figure 4-7. The permeability and porosity Case 1a and 1b are shown in Figure 4-8. Production was specified to occur at a target oil rate of 3,000 STB/D in both cases with a minimum bottom hole pressure of 1800 psi.

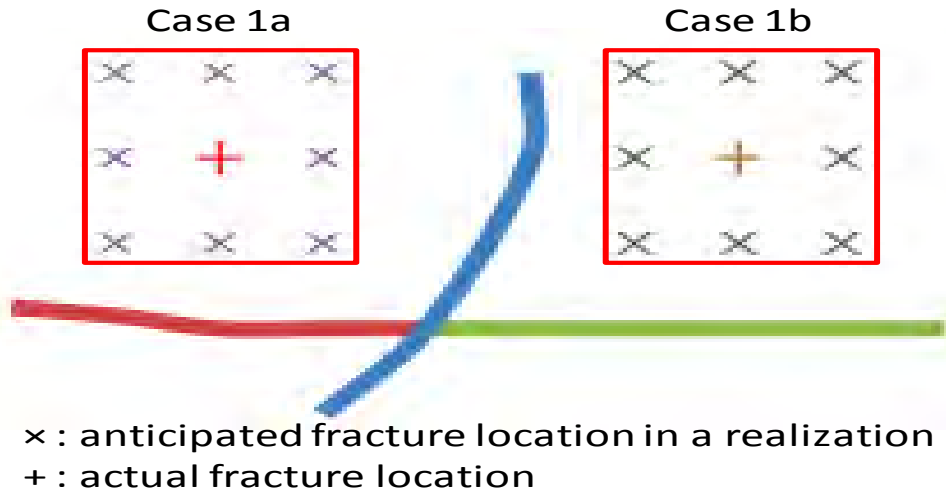


Figure 4-7: location of study areas in Case 1a and Case 1b

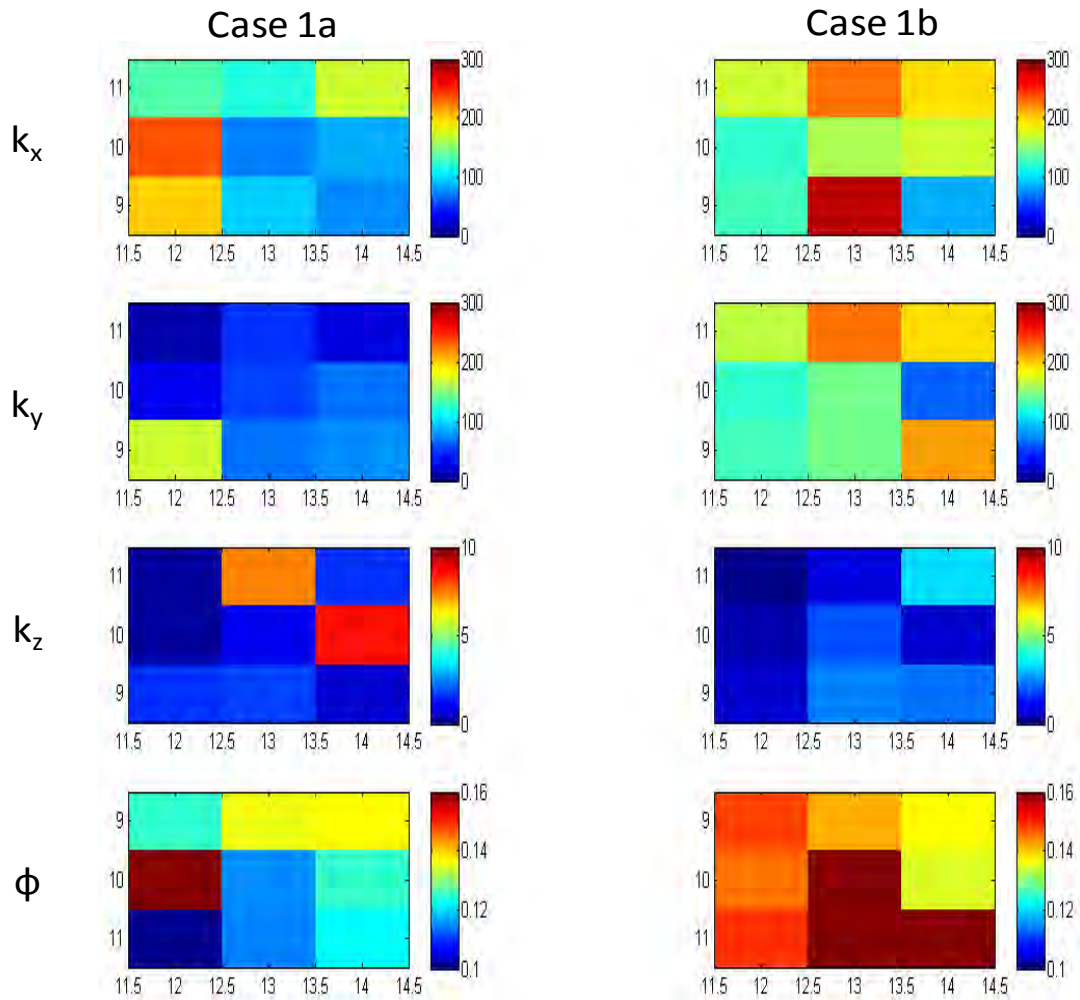


Figure 4-8: Onshore model - permeability and porosity of Case 1a and Case 1b

4.4.1. Onshore Model – Case 1a

GA was run for three generations with a total population size of nine to maximize the objective function, which is NPV in this case. The expected NPV was compared to its respective base case as in Table 4-1. The base case corresponded to the case where the location of the fracture was known. This table indicates that the optimization was not affected by the location of the fracture as long as the fracture remained within the highlighted area in Figure 4-7. The reason for this is that water production that affected the motherbore and lateral-3 (indicated by the ICV restriction) was due mostly to the advancement of the waterflood front. Although the fractures accelerated water production, water production was overwhelmed by the waterflood front advancement. The difference in the optimum ICV configuration in Case 1a and its corresponding base cases was small (within GA error). It is worth noting that the ICVs were set at a higher position to increase NPV as the horizontal permeability was relatively lower. The difference in NPV was also very small which confirms the insensitivity of this case to the location of the fracture.

Table 4-1: Comparison of fracture location effect – case 1a

	NPV	Optimum ICV	Difference
<i>Base case 1a</i>	\$622,958,763	(4 5 1)	0.0%
<i>Case 1a</i>	\$612,538,543	(4 5 0)	1.7%

4.4.2. Onshore Model – Case 1b

Similar to Case 1a, GA was run for three generations with a total of nine individuals in each population to maximize the NPV which is the comparison basis. Although Case 1b shows better horizontal permeability and porosity in general which might increase the effect of fractures in transmitting water to the production well, it was found out that this case is also insensitive to the fracture location as long as the fracture is within the highlighted area in Figure 4-7. The water

production in this case was coming due to waterflood front from the west and fractures from the east. However, the fractures did not seem to alter the optimum ICV configuration even though the expected NPV was lowered by 1.4%. In fact the difference in NPV between Case 1b and its corresponding base case is only 1.4%, Table 4-2.

Table 4-2: Comparison of fracture location effect – case 1b

	NPV	Optimum ICV	Difference
<i>Base case 1b</i>	\$603,487,630	(4 7 1)	0.0%
<i>Case 1b</i>	\$595,235,488	(5 7 1)	1.4%

4.5. Onshore Model Fracture Study – Case Two

This case is very similar to Case one. However, the source model DFNs were arranged to occupy bigger areas as shown in Figure 4-9 for Case 2a and Case 2b. In addition, the base cases were simulated twice with the actual fracture in different locations within the candidate fracture area. The permeability and porosity of both cases are given in Figure 4-10.



× : anticipated fracture location in a realization
 + : actual fracture location

Figure 4-9: location of study areas in Case 2a and Case 2b

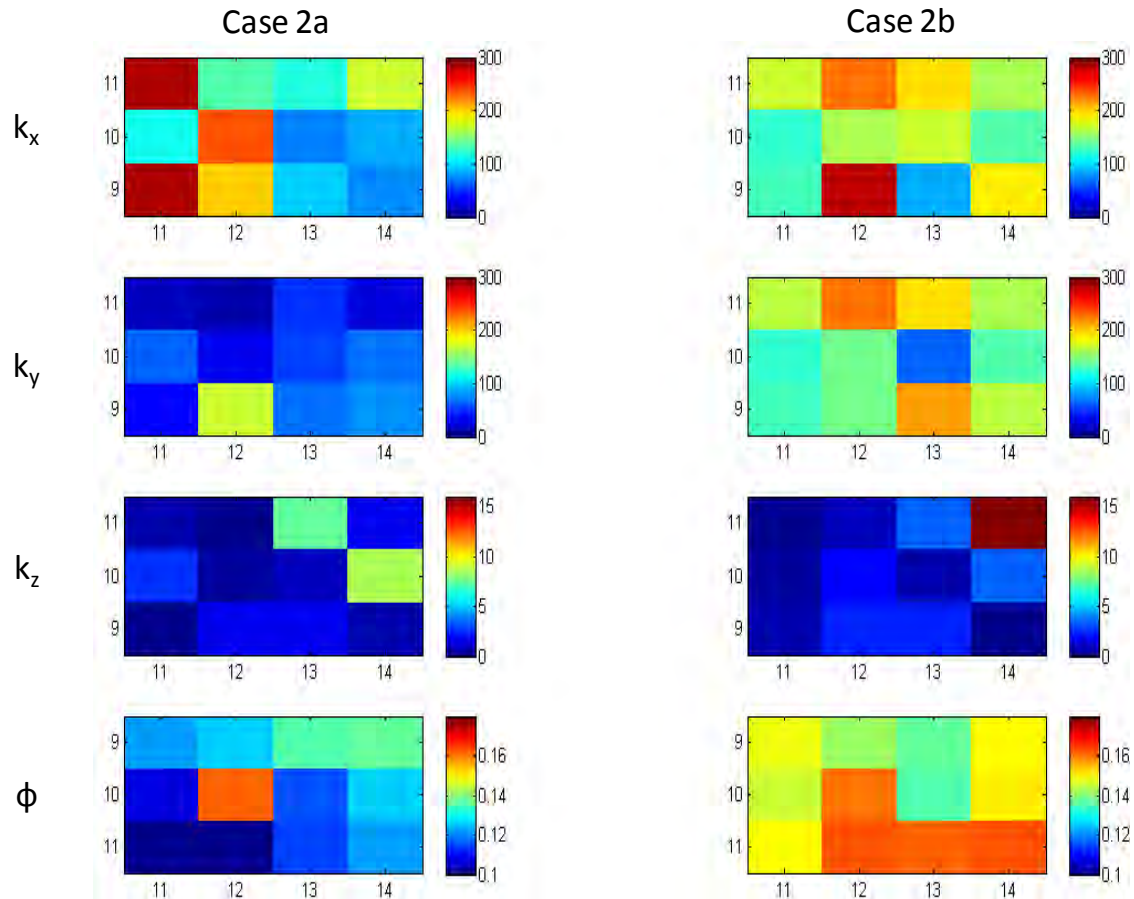


Figure 4-10: Onshore model - permeability and porosity of case 2a and case 2b

4.5.1. Onshore Model - Case 2a

The expected NPV which comprised the average value for fracture locations around the boundary of the candidate area was compared against the NPVs resulted from the fracture located at grid blocks (12,10) and (13,10). Table 4-3 summarizes the difference between Case 2a and the base cases. It can be seen that the difference in NPV was very small as most of the water production was due to waterflood front advancement.

Table 4-3: Comparison of fracture location effect – case 2a

	NPV	Optimum ICV	Difference
<i>Base case (12,10)</i>	\$627,788,988	(4 5 0)	0.0%
<i>Base case (13,10)</i>	\$622,958,763	(4 5 1)	0.8%
<i>Case 2a</i>	\$623,435,899	(4 5 0)	0.7%

4.5.2. Onshore Model – Case 2b

Now we look at Case 2b where the area of study is located east of the well as in Figure 4-9. Comparing the NPV from Case 2b and the base case where the fracture is located at grid block (18,10), we can see a minor difference of 0.97% in NPV. In addition, the ICV of lateral-1 which in this case sees water production from both sides did not change. However, the difference in NPV between Case 2b and the base case where the fracture is in grid block (19,10) rose to 4.9%. This difference altered the optimum ICV configuration as evident from Table 4-4. The optimum ICV changed to (6 7 1) as the fracture was placed further away from lateral-1 and therefore water production brought by the fracture was minimized.

Table 4-4: Comparison of fracture location effect – case 2b

	NPV	Optimum ICV	Difference
<i>Base case (18,10)</i>	\$603,487,630	(4 7 1)	0.0%
<i>Base case (19,10)</i>	\$632,945,410	(6 7 1)	4.9%
<i>Case 2b</i>	\$609,367,689	(4 5 0)	0.97%

Knowing the exact location of the fracture was not essential in Cases 1a and 2a. The reason for this is that water production was mostly caused by the advancement of the waterflood front. The fractures slightly accelerated water production. In Cases 2a and 2b, the fractures were far away from the waterflood front. Although water production was caused by the advancement of floodfront and the fracture in Case 1b, the optimum ICV configuration remained unchanged due to the small candidate area. The difference in NPV between Case 1b and its

corresponding base case was only 1.4%. However, the difference between Case 2b and its corresponding base case was 4.9%. This difference altered the optimum ICV configuration from (4 5 0) to (6 7 1) as the fracture was placed further away from the production well and therefore water production brought by the fracture was minimized. Hence, knowing the exact location of the fracture in Case 2b was very important to the optimization process.

CHAPTER 5

5. Conclusions and Future Work

5.1. Conclusions

A general methodology was used to optimize production from smart wells. The methodology entailed the use of genetic algorithm applied in conjunction with a commercial reservoir simulator that is capable of simulating ICVs. The methodology utilized a built-in data library to reduce the number of required runs to find the optimum ICV configuration.

The general algorithm was applied to several field cases with different objectives. ICVs were designed for each case to ensure that each setting yielded different production rates and therefore significantly impacted the optimization process. Different objectives were achieved using the algorithm. These objectives include minimizing water cut, extending production plateau, and maximizing NPV. Applying the algorithm in one case resulted in an extended production plateau of six years as opposed to four years when using the current ICV configuration.

The leveraged knowledge gained from working these different cases has provided an insight into the effect of heterogeneity on the optimization methodology. A technique was proposed to quantify the effect of fractures on the optimization process. Various reservoir realizations were created to study and quantify the impact of fractures on the production optimization process. One case concluded that knowing the fracture location did not affect the optimum ICV configuration when it was generally close to the injected water floodfront. However, the fracture location altered the optimum ICV configuration when it was on the opposite side from the water floodfront.

5.2. Future Work

The following items are proposed to improve the optimization of smart wells production:

- Additional search algorithms can be hybridized with GA to increase the efficiency and speed of the optimization method.
- The optimization methodology can be modified to handle the change of ICV configuration with time.
- Rea-time data such as pressure and temperature can be used as evaluation parameters to provide continuous production optimization. Smart completions are often equipped with this kind of real-time sensors.

Nomenclature

Abbreviations

BHP	well bottom hole pressure
DFN	discrete fracture network
FVF	formation volume factor
GA	genetic algorithm
ICV	inflow control valve
NCW	nonconventional well
NPV	net present value
OWC	oil water contact
PI	productivity index
WC	water cut
WI	well index
E	expected value

Variables

A_c	area of constriction
A_p	area of pipe
ρ	density
D	diameter of well
f	fanning friction factor
L	length of tube
q_m	mixture flowrate
p_m	mutation probability
k	permeability
k_r	relative permeability

Bibliography

Aguilera, R., *Naturally Fractured Reservoirs*, PennWell Books, Tulsa, Oklahoma, 521 p., 1995

Alhuthali, A. H., Datta-Gupta, A., Bevan, Y., Fontanilla, J. P., (2009). Field Applications of Waterflood Optimization via Optimal Rate Control With Smart Wells, paper SPE 118948 presented at the SPE Reservoir Simulation Symposium in Woodland, Texas, U.S.A., 2-4 February

Brouwer, D. R. and Jansen, J.D. (2002). Dynamic Optimization of Water Flooding with Smart Wells Using Optimal Control Theory, paper SPE 78278 presented at the SPE European Petroleum Conference, Aberdenn, UNITED KINGDOM, 29-31 October.

Dumville, J. "Smart Well Graph." E-mail to Zeid Ghareeb. 5 April 2008.

Guyaguler, B. (2002). *Optimization of Wells Placement and Assessment of Uncertainty*. PhD dissertation, Department of Petroleum Engineering, Stanford University, California.

HLS Asia Limited. 25 May 2009 < <http://www.hlsasia.com/servopenhole5.htm>>.

Jalali, Y., Bussear, T., and Sharma, S. (1998). Intelligent Completions Systems – The Reservoir Rationale, paper SPE 50587 presented at the SPE European Petroleum Conference, The Hague, Netherlands, 20-22 October.

Mavko, G., Mukerji, T., Dvorkin, J., *The Rock Physics Handbook*, Cambridge University Press, 1998

Mubarak, S. M., Pham, T. R., Shamrani, S. S., and Shafiq, M. (2007). Using Down-Hole Control Valves to Sustain Oil Production From the First Maximum Reservoir Contact, Multilateral and Smart Well in Ghawar Field: Case Study, paper IPTC 11630 presented at the International Petroleum Technology Conference in Dubai, U.A.E., 4-6 December.

Voelker, J. (2004). *A Reservoir Characterization of Arab-D Super-K as A Discrete Fracture Network Flow System, Ghawar Field, Saudi Arabia*. PhD dissertation, Department of Petroleum Engineering, Stanford University, California.

Warren, J. E., Root, P. J., (1963). The Behavior of Naturally Fractured Reservoirs. SPE Journal, 3 March.

Yeten, B. (2003). *Optimum Deployment of Nonconventional Wells*. PhD dissertation, Department of Petroleum Engineering, Stanford University, California.

Yeten, B., Durlafsky, L. J., Aziz, K., (2002). Optimization of Smart Well Control, paper SPE/PS-CIM/CHOA 79031 presented at the SPE International Thermal Operations and Heavy Oil Symposium and International Well Technology Conference in Calgary, Alberta, CANADA, 4-7 November

Appendix A

Optimization Code

This section explains the code used to find out the optimum ICV setting. GA MATLAB was used as the main engine for the optimization. GA MATLAB can be thought of as a loop that sends certain values to a main function and receives the results. Certain operations are performed such as crossover and mutation on the results to generate the second set of values. GA MATLAB contacts only one main function called `call_ecl` that runs Eclipse and brings the results back to GA MATLAB. Other functions used include `control_write` and `control_read` to enter inputs and evaluate outputs.

GA MATLAB

Lower and upper boundaries definition:

```
LB = logical([0 0 0 0 0 0 0 0 0]);  
UB = logical([1 1 1 1 1 1 1 1 1]);
```

GA options such as number of generations, population size, mutation function,...
etc:

```
options = gaoptimset;  
options = gaoptimset(options, 'Generations', gen);  
options = gaoptimset(options, 'populationSize', pop);  
options = gaoptimset(options, 'EliteCount', 1);  
options = gaoptimset(options, 'PopulationType', 'bitString');  
options = gaoptimset(options, 'StallGenLimit', Inf);  
options = gaoptimset(options, 'MutationFcn', {@mutationuniform, rate});  
options = gaoptimset(options, 'FitnessScalingFcn', @fitscalingrank);  
options = gaoptimset(options, 'SelectionFcn', @selectionroulette);  
options = gaoptimset(options, 'CrossoverFraction', n);
```

GA execution code that uses the main function to run Eclipse and receive the results:

```
[scores] = ga(@call_ecl, 9, [], [], [], [], [], options);
```

Main Routine

The main routine is responsible for supplying ICVs to Eclipse, reading results, and sending them to GA MATLAB.

Sending the ICVs given by GA MATLAB to the simulator

```
control_write('valvecontrol.dat',x)
```

Running Eclipse

```
dos('$Eclipse ECL_RUN1 > ecloutput.dat');
```

Reading the results

```
[WC]=control_read('ECL_RUN1.RSM', columns_number1);
```

Closing Eclipse

```
dos('del ECL_RUN1.RSM');
```

Writing Function

This function is responsible for converting ICV settings to the corresponding areas, and then writing them in the simulator file.

Converting the ICV settings to the corresponding areas

```
if x(1) == 0
    y1 = 1e-12;
elseif x(1) == 1
    y1 = 0.000038;
elseif x(1) == 2
    y1 = 0.00008;
elseif x(1) == 3
    y1 = 0.00013;
elseif x(1) == 4
    y1 = 0.00019;
elseif x(1) == 5
    y1 = 0.00027;
elseif x(1) == 6
    y1 = 0.00038;
elseif x(1) == 7
    y1 = 0.00057;
end
```

Similar work is done for ICV2 and ICV3.

Writing the areas in the simulator file

```
fid = fopen(fle, 'w');

fprintf(fid, 'WSEGVAlV \n');
fprintf(fid, ' ''PRODZ'' 2 0.686 %g/ \n', y1);
fprintf(fid, '/ \n');

fprintf(fid, 'WSEGVAlV \n');
fprintf(fid, ' ''PRODZ'' 5 0.686 %g/ \n', y2);
fprintf(fid, '/ \n');

fprintf(fid, 'WSEGVAlV \n');
fprintf(fid, ' ''PRODZ'' 8 0.686 %g/ \n', y3);
fprintf(fid, '/ \n');
```

Reading function

```
fid = fopen(fle, 'r');
```

This loop is used to discard comment lines in the simulator output file

```
for i = 1:10
    tline = fgetl(fid);
end
```

Reading the data and converting them to a matrix

```
m = fscanf(fid, '%f'); % reads data from choke.RSM and format as text
n1 = reshape(m, columns_number1, length(m)/columns_number1);
n1 = transpose(n1);

fclose(fid);
```

Appendix B

The Simulator

Eclipse simulator was used to simulate all the cases presented in this report. It is worth mentioning how multilateral wells and ICVs are presented in the simulator. Multilateral wells consist of three main records. They are explained below.

This record defines the laterals, how many segments they include, and the length of each segment. In this example, there are three laterals. Each lateral include one segment that is 500 feet.

```
WELSEGS
--      TVD      MD
'PRODZ' 8000    0 1e-005 'ABS' 'HFA' 'HO'/
2 2 1 1500      8000    0.17 0.001 0.0226980069221862 54.456/
3 3 2 1 500     8000    0.17 0.001 0.0226980069221862 54.456/
4 4 3 1 500     8000    0.17 0.001 0.0226980069221862 54.456/
```

/

The grid blocks that the well intersects are shown here. Each lateral intersects two grid blocks in this example.

```
COMPDAT
'PRODZ' 20 20 1 1 OPEN 0 0 0.34 0 0/
/
COMPDAT
'PRODZ' 21 21 1 1 OPEN 0 0 0.34 0 0/
/
COMPDAT
'PRODZ' 19 20 1 1 OPEN 0 0 0.34 0 0/
/
COMPDAT
'PRODZ' 18 20 1 1 OPEN 0 0 0.34 0 0/
/
COMPDAT
'PRODZ' 21 19 1 1 OPEN 0 0 0.34 0 0/
/
COMPDAT
'PRODZ' 22 18 1 1 OPEN 0 0 0.34 0 0/
/
```

The relationship between the grid blocks and the individual lateral is shown here. In this example, each lateral intersects two grid blocks. The length of each intersected block is 250 ft.

```
COMPSEGS
'PRODZ' /
20 20 1 1 0 250 'Y' 3* /
21 21 1 1 250 500 'Y' 3* /
19 20 1 2 0 250 'Y' 3* /
```

```
18 20 1 2    250  500 'Y' 3* /
21 19 1 3    0   250 'Y' 3* /
22 18 1 3    250  500 'Y' 3* /
/
```

This record defines the ICVs for this well.

```
INCLUDE
'valvecontrol.dat' /
```

The well's target is defined.

```
WCONPROD
      PRODZ   OPEN  ORATE   300   1*   1*   1*   1*   0 /
/
```

The economic limit of the well is defined.

```
WECON
'PRODZ' 100 1* 0.98 1* 1* 'NONE' 'NO' /
/
```